

## Intelligent micellar polymeric nanocarriers for therapeutics and diagnosis

Antonio Topete,<sup>1</sup> Silvia Barbosa,<sup>2</sup> Pablo Taboada<sup>2</sup>

<sup>1</sup>Laboratorio de Inmunología, Departamento de Fisiología, Centro Universitario de Ciencias de la Salud, Universidad de Guadalajara, 44340 Guadalajara, Jalisco, Mexico

<sup>2</sup>Grupo de Física de Coloides y Polímeros, Departamento de Física de la Materia Condensada, Universidad de Santiago de Compostela, 15782 Santiago de Compostela, Spain

Correspondence to: P. Taboada (E-mail: pablo.taboada@usc.es)

**ABSTRACT:** Polymeric micelles can be designed and synthesized to bear polymeric blocks with different hydrophilicities; this triggers their self-assembly into micellar aggregates similar to those generated with traditional surfactants. The basic structure consists of a hydrophobic core, capable of containing guest substances, and a hydrophilic shell, which stabilizes the payload and protects it from external degradation or prevents its quick elimination from the body. The accumulation of block copolymer micelles (BCMs) in a target cell or tissue can be accomplished by two main mechanisms, passive and active targeting; this allows the payload release at the site of action when desired. Hence, in this general overview, we pay special attention to newly developed single-stimulus- and multi-stimuli-responsive delivery systems capable of disassembling and reassembling (in some cases) as a response to changes in their physicochemical properties. Also, special interest is also devoted to multifunctional BCMs incorporating multiple therapeutic agents and/or multiple imaging contrast agents, which can be considered the new generation (third generation) of drug-delivery systems, that is, nanotheranostic platforms. Finally, a summary of BCM-based drug-delivery systems currently under clinical trials is given. © 2015 Wiley Periodicals, Inc. *J. Appl. Polym. Sci.* **2015**, *132*, 42650.

**KEYWORDS:** biomedical applications; biomaterials; copolymers; drug-delivery systems; self-assembly

Received 24 April 2015; accepted 17 June 2015

DOI: 10.1002/app.42650

### INTRODUCTION

During the last 2 decades, a large number of new nanotechnology-based ideas and proofs of concept for diagnosis and therapeutics have emerged, and their feasibility has been demonstrated.<sup>1–3</sup> Considerable attention has particularly been focused on nanotechnology-based drug delivery to overcome current problems associated with systemic chemotherapy, such as the use of high drug concentrations to achieve optimal therapeutic tissue concentrations and their related systemic toxicities. The incorporation of chemotherapeutic agents into nanosized drug carriers has several potential advantages compared to systemic chemotherapy: (1) enhanced bioavailability, (2) increased circulation times, (3) avoidance of toxic solubilizing adjuvants for administration, and (4) use of lower drug concentrations, among others. To obtain such benefits, the design of nanosized drug carriers must meet some criteria. The first one is the consideration of how to encapsulate and release drugs because these payloads should be retained stably within the nanocarrier until they reach the target organs, tissues, cells, or intracellular organelles to maximize their therapeutic effect and minimize off-target ones. Drug-delivery nanosystems should also

allow time-dependent drug distribution in the body (biodistribution) for improved therapeutic effectiveness and reduction of associated toxic effects. To reach these goals, the intended administration route of the nanocarrier must be also considered in its design to fulfill efficient payload encapsulation, release, and correct biodistribution. For example, nanocarriers for oral administration must be resistant to the harsh conditions found in the gastrointestinal tract, particularly the acidic environment of the stomach, and must adhere to the intestinal mucosa and cross the mucus layer to the epithelium for payload absorption.<sup>4</sup> Conversely, for systemic intravenous administration, the size and surface properties of the nanocarriers must be carefully designed to prevent renal clearance and capture by the reticuloendothelial system.<sup>5</sup>

Polymer–drug carriers, including polymer–drug conjugates and polymeric micelles, have proven to meet the former criteria, and several formulations have been already entered clinical trials.<sup>6</sup> In particular, block copolymer micelles (BCMs) possess several basic advantages in their characteristics: (1) a spontaneous formation process from the self-assembly of copolymer chains in water and a unique core–shell structure; (2) the

**Antonio Topete** obtained a M.S degree in chemical engineering from the University of Guadalajara, Mexico. He was granted by Mexico's National Council of Science and Technology a scholarship to study at the University of Santiago de Compostela, Spain, where he obtained a Ph.D. degree in materials science. His research work is centered on the development of multifunctional theranostic nanoplatfoms made from polymeric, biological, and inorganic materials and their applications in biomedical and biotechnological areas. Recently, he was granted a National Council of Science and Technology's Repatriation Program fellowship, and he is currently working at the University of Guadalajara as an associate researcher-professor.



**Silvia Barbosa** completed her Ph.D. in Materials Science at the University of Santiago de Compostela in 2005. Next, she held postdoctoral positions at the University of Pais Vasco with Issa Katime in 2005 and 2006 and Steve G. Yeates at the University of Manchester from 2006 to 2008. In 2008, she joined Luis Liz-Marzan's group with a Juan de la Cierva fellowship for 2 years. Currently, she is working as a Ramón y Cajal Research Associate at the Condensed Matter Physics Department in the University of Santiago de Compostela. Her current interests involve the development of theranostic nanoplatfoms for biomedical applications and ordered assemblies of metallic nanoparticles from block copolymer nanolithography for biosensing applications.



**Pablo Taboada** obtained his Ph.D. in materials science from the University of Santiago de Compostela in 1999 and has been a postdoc at University of Manchester. He moved back to the University of Santiago de Compostela again in 2001 as a Ramón y Cajal Research Associate, where he is currently associate professor with full professorship habilitation. He is coauthor of over 140 publications and has received several research acknowledgments. His current research interests include the self-assembly processes of hybrid polymeric materials for drug delivery and tissue engineering and the design of nanostructured materials (nanoparticles and thin films) for theranostic, sensing, and energy applications.



micellar hydrophobic core may serve as a solubilization depot for drugs with poor aqueous solubility, whereas the hydrophilic shell surrounding the core provides protection to the cargo; and (3) a small micellar size (from 10 to about 200 nm) with a narrow size distribution, which allows efficient cell internalization. Additionally, the synthetic polymeric chains forming the micelle allow for the fine tuning of their chemistries; this can dramatically improve the functional outcomes of BCMs as needed for their use as drug-delivery systems.<sup>7-9</sup> In this regard, new drug-delivery systems have been developed on the basis of stimuli-responsive BCMs capable of switching the release of their cargo on and off by internal or external induction (temperature and pH changes, light, ultrasound, etc.). In this article, we give a brief description of the main features of BCMs, which allow their use as delivery nanovehicles designed for drug solubilization, transport, and release. Next, we focus specifically on the main principles of designing stimuli-responsive and multifunctional BCMs, highlighting some of the most relevant advances during the last years on this new generation of nanocarriers. We conclude with a prospective outlook at future trends in the field.

#### POLYMERIC MICELLES: MICELLIZATION AND STRUCTURE

The hydrophobic core-hydrophilic shell nanostructure of BCMs is formed at a concentration termed the *critical micelle concen-*

*tration* (cmc). The micellar core serves as a reservoir for poorly aqueous soluble drugs because of their tendency to partition into it as a result of predominant hydrophobic interactions. The core can sometimes be made up of a water-soluble polymer that is rendered hydrophobic by chemical conjugation of a water-insoluble drug<sup>10</sup> or by complexation of two oppositely charged polyions to give the so-called polyion complex micelles.<sup>11</sup> In terms of the hydrophobic core composition, biocompatibility, solubility, stability, release rate, and nontoxicity are key prerequisites in selecting the appropriate hydrophobic segment. Commonly used core-forming hydrophobic polymers for drug delivery can be poly(oxide ether)s, such as poly(propylene oxide) (PPO) in Pluronic<sup>12</sup> and Tetronics<sup>13</sup> copolymers, poly(butylene oxide) (PBO),<sup>14</sup> poly(styrene oxide) (PSO),<sup>15</sup> or poly(phenyl glycidyl ether) (PG);<sup>16</sup> polyesters, such as poly(lactic acid) (PLA),<sup>17</sup> poly(lactide-co-glycolic acid) (PLGA),<sup>18</sup> and poly( $\epsilon$ -caprolactone) (PCL);<sup>19</sup> poly(L-amino acids), such as poly(L-lysine) (PLys);<sup>20</sup> and phospholipids and lipid derivatives, such as distearyl phosphatidyl ethanolamine.<sup>21</sup>

The shell around the core acts as a physical shield that stretches away from the core because of geometrical constraints and limits its interaction with the external milieu; this stabilizes the system. The corona also constitutes the interface between the drug reservoir and the release medium; depending on its properties

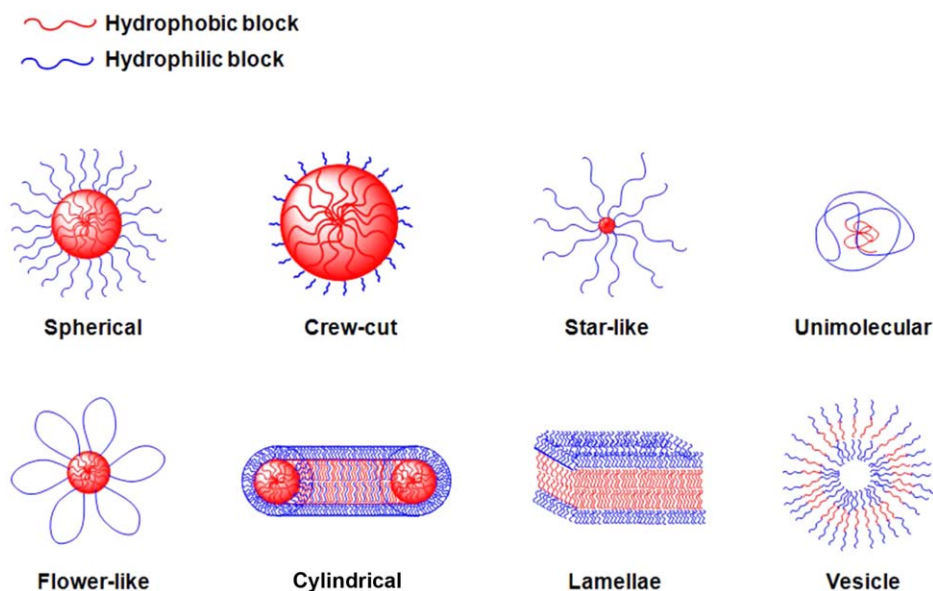


**Figure 1.** Different geometrical shapes acquired by BCs. They depend on the block length, solvent, temperature, pH, and so forth. [Color figure can be viewed in the online issue, which is available at [wileyonlinelibrary.com](http://wileyonlinelibrary.com).]

(e.g., microfluidity) and on drug–corona interactions, the drug release can be facilitated or hampered.<sup>9</sup> As the shell-forming block, several hydrophilic and nonionic polymers, such as poly(ethylene glycol) (PEG),<sup>18,22</sup> poly(ethylene oxide) (PEO),<sup>23</sup> poly(*N*-vinyl pyrrolidone),<sup>24</sup> poly(2-oxazoline),<sup>25</sup> poly(*N*-isopropyl acrylamide) (PNIPAAm),<sup>26</sup> and poly(hydroxypropyl methacrylamide),<sup>27</sup> have been reported. Among them, PEG is the most frequently used for several reasons, including the following: (1) its excellent solubility in aqueous media and several organic solvents, which allows for flexibility in preparation procedures; (2) nontoxicity and low immunogenicity; and (3) lack of interaction with biological components; this provides stealthiness and prevents uptake by the reticuloendothelial system and allows longer circulation times *in vivo*.<sup>28</sup>

The mechanism of micellization and the structural and physicochemical properties of BCs, including their size, shape, and nature and strength of drug–micelle interactions, are results of the interplay of several different factors, including the deformation of the hydrophobic blocks, the surface tension between the hydrophobic blocks and the solvent, and the interactions among the block copolymer chains during micelle formation.<sup>29</sup> These features can be tailored by selecting and adjusting the copolymer architecture (linear, branched, star-shaped, etc.), chemical nature (polarity, electric charge, pendant groups, etc.) of the forming blocks, solvent quality, presence of additives, and solution temperature. For example, the micellization of block copolymers bearing both nonionic hydrophobic and hydrophilic blocks, such as PEO,<sup>23</sup> poly(2-oxazoline),<sup>25</sup> PNIPAAm,<sup>26</sup> and poly(vinyl ether),<sup>30</sup> is mainly driven by hydrophobic forces; these are largely controlled by the hydrophobic block length.<sup>14</sup> Hydrogen bonding and metal–ligand coordination interactions can also play an important role.<sup>31,32</sup> Poloxamers composed of PEO and PPO blocks, both of which are water soluble below 15°C, experience an enhancement in their hydrophobicity as the temperature is raised because the PPO block is more sensitive

and eventually triggers micellization.<sup>14</sup> Conversely, the micellization process of block copolymers bearing one ionic or ionizable block, including poly(4-vinyl pyridinium alkyl halide),<sup>33</sup> poly(methyl acrylate),<sup>34</sup> poly(methyl methacrylate),<sup>35</sup> poly(styrene sulfonate),<sup>36</sup> polypeptide blocks such as poly(arginine),<sup>37</sup> PLys,<sup>20</sup> poly(aspartic acid) (PAsp),<sup>38</sup> or polydendritic charged blocks,<sup>39</sup> is additionally governed by the repulsive electrostatic interactions between charged polymer units; this makes these BCs sensitive to subtle changes in the physicochemical properties, such as the pH or temperature, of the surrounding medium and, hence, appropriate for controlled drug delivery.

In general, BCs in aqueous solutions are usually spherical with narrow size distributions, but changes in their shape and size may occur under certain conditions. Crew-cut and starlike shapes are two typical configurations of spherical micelles (Figure 1). The first structure is usual for copolymers bearing long hydrophobic and short hydrophilic blocks, whereas starlike structures are commonly observed for block copolymers with long hydrophilic and short hydrophobic chains and in starlike ionic copolymers.<sup>40</sup> When a block copolymer bears long hydrophobic blocks, highly hydrophobic monomers (e.g., PSO or PG) or long asymmetric structures, the insoluble aqueous block acquires a collapsed conformation protected by the hydrophilic one; this decreases its interactions with water. This structure is referred to as *unimolecular micelles*.<sup>41</sup> Triblock copolymers with short hydrophobic end blocks (called *telechelics*) may be prone to associating into flowerlike micelles, in which hydrophilic middle blocks are looped.<sup>42</sup> The bridging of these micelles occurs when the middle block spans the space between different micelles. Furthermore, when the micelle core radius exceeds the stretched length of the hydrophobic block, cylindrical, lamellar, and vesicular structures (polymersomes) can be formed.<sup>43–46</sup> Transitions from spherical to other shapes has been observed to be triggered by changes in solvent temperature or polarity or the presence of additives, such as salts or homopolymers,<sup>43–45</sup> as

noted, for example, for nonionic PEO–PPO–PEO.<sup>43</sup> Other more exotic micellar structures, such as core–shell–corona (onion-like),<sup>46</sup> pointed-oval-shaped,<sup>47</sup> disk-shaped,<sup>48</sup> toroidal (doughnutlike),<sup>49</sup> double-faced (Janus-type),<sup>50</sup> and bicontinuous<sup>51</sup> BCMs, have also been observed and studied. Although most BCMs designed as drug carriers are spherical, micelles with a more hydrodynamic shape, such as ellipsoidal or disklike ones (mimicking the morphology of natural biological transporters, e.g., erythrocytes), might be more efficient in transporting their cargo through the bloodstream and delivering it to the site of action. Although nonspherical shapes are thermodynamically disfavored,<sup>48</sup> the crosslinking of the micellar core or shell could be an efficient strategy for overcoming this problem.<sup>52</sup> Moreover, if crosslinking can be reversed by a stimulus (e.g., pH, light),<sup>53</sup> controlled and selective delivery of the drug might be also attainable.

## POLYMERIC MICELLES AS DRUG NANOCARRIERS

### Drug Solubilization by BCMs

To achieve enhanced physical entrapment of poorly aqueous soluble drugs inside micellar cores, a required condition is the existence of good compatibility between the hydrophobic core and the drug molecule; this can be achieved by ensuring a structural similarity and/or polarity between the drug molecule and the hydrophobic part of the copolymer. As such, micelles composed of PEG–poly(vinyl benzyl oxy-*N,N*-diethyl nicotinamide) can yield BCMs exhibiting hydrotropic properties toward the antineoplastic drug paclitaxel (PTX). Micelles of this copolymer can accept up to 37.4% w/w of this compound;<sup>54</sup> this, thereby, raises the aqueous solubility of the drug to 38.9 mg/mL instead of less than 1 µg/mL of the free drug in water. Other factors, such as the hydrophilic–lipophilic balance, the polymer molecular weight, block lengths, compactness of the micellar core, and drug–polymer ratio also play an important role in the drug solubilization process. For example, drug loading can be tuned by replacing a PPO inner block with a more hydrophobic one, such as PBO, PSO, or PG. In this manner, the micelles of the copolymer EO<sub>137</sub>SO<sub>18</sub>EO<sub>137</sub> (the subscripts denote the respective block lengths) have been shown to solubilize five times more of the antifungals griseofulvin, quercetin, and rutin than Pluronic EO<sub>62</sub>PO<sub>39</sub>EO<sub>62</sub>; mixed micelles led to intermediate solubilization capabilities.<sup>55</sup> EO<sub>*m*</sub>SO<sub>*n*</sub>EO<sub>*m*</sub> triblock copolymers with longer SO blocks have also demonstrated larger effective drug loading than those with shorter SO segments.<sup>15</sup> Nevertheless, a compromise between the chain solubility and micellar core size must be attained by the tuning of the EO and SO block lengths, with an empirical optimal EO–SO ratio found at about 1.5.<sup>15</sup> Furthermore, the influence of the amount of feeding drug on the encapsulation yield was also largely evidenced.<sup>15–56</sup>

In addition to hydrophobic interactions, polymeric micelles can also entrap drugs through other approaches, such as the covalent conjugation of the drug to the polymer by means of nonlabile or labile bonds before the formation of micelles.<sup>57</sup> Metal complexes, such as platinum (cisplatin, carboplatin, etc.), iron (ferrocenium pricate and trichloroacetate), cobalt [cobalt(III) complexes] or ruthenium [Ru(III) complexes, e.g., NAMI-A and

KP1019) can be also incorporated into ligating polymers through the ligand exchange of one or more ligand groups at the metal center.<sup>58</sup> The incorporated metal complexes can contribute to the enhancement of the polymer hydrophobicity and crosslink the blocks; this leads to micelle core stabilization. The entrapment of hydrophilically charged molecules such as proteins and nucleic acids can be reached by the exploitation of electrostatic interactions and charge neutralization between the macromolecules and oppositely charged core-forming blocks, such as polyethylenimine (PEI), PLys, or PAsp; this leads to the formation of core-loaded polyion complex micelles.<sup>59</sup> On the other hand, the solubilization and stabilization of a drug that can be otherwise damaged by a hydrolytic or proteolytic environment into a micelle core may protect the drug from such a hostile environment to some degree, in a manner analogous to drug encapsulation by semipermeable membranes. For example, micelles composed of a triblock PAA–PCL–PAA copolymer have been shown to solubilize and stabilize the lactone form of the cytotoxic drug camptothecin because of the ability to incorporate these molecules not only into the PCL core but also in the PAA shell. The encapsulation of this drug inside the BCMs notably hindered the hydrolytic opening of the lactone ring of camptothecin in aqueous and biological media.<sup>60</sup>

### Micellar Stability

To ensure both the stability and delivery of the payload to its site of absorption, a micellar nanocarrier must be able to resist rapid dissociation upon dilution and exposure to the biological milieu. Differently from micelles of conventional surfactants, BCMs exhibit much lower cmc's and, thus, show a greater resistance to dissociation by dilution when the micelle is introduced in a physiological environment.<sup>61</sup> For example, cmc's in the range of micromoles per liter were obtained for different PEO–PBO, PEO–PSO,<sup>14</sup> or poly(*N*-decyl acrylamide)–poly(*N,N*-diethyl acrylamide) based block copolymers, for example,<sup>62</sup> whereas cmc's in the range of millimoles per liter were determined for different sodium alkyl sulfates,<sup>63</sup> alkyl–trimethyl ammonium bromides,<sup>64</sup> and nonionic surfactants of the Brij, Tween, and Triton X families.<sup>65</sup> In addition to thermodynamic stability, polymeric micelles also show a marked kinetic stability because of the slow-exchange kinetics of unimers between the micelles and bulk chain solution, and therefore, they do not instantaneously release the encapsulated drug but do so in a sustained way that prevents the risk of drug precipitation–degradation.

As for drug solubilization, the micellar stability can be enhanced by either construction of polymers with more hydrophobic blocks or an increase in the hydrophobic chain length in a constant corona chain-forming block. Indeed, the micelles of the EO<sub>33</sub>SO<sub>14</sub>EO<sub>33</sub> copolymer have been shown to display a greater stability than those of its counterpart EO<sub>38</sub>SO<sub>10</sub>EO<sub>38</sub> in a cell culture; they mimic conditions retaining about 80% of the encapsulated drug after 20 days of incubation without significant changes in the micellar size.<sup>57</sup> Copolymers of the type EO<sub>*m*</sub>SO<sub>*n*</sub>EO<sub>*m*</sub> have also been shown to be more stable against dilution than their EO<sub>*m*</sub>PO<sub>*n*</sub>EO<sub>*m*</sub> Pluronics and Tetronics counterparts.<sup>56,66</sup> Conversely, when the hydrophilic block length is decreased and the hydrophobic block is unaltered, a stability



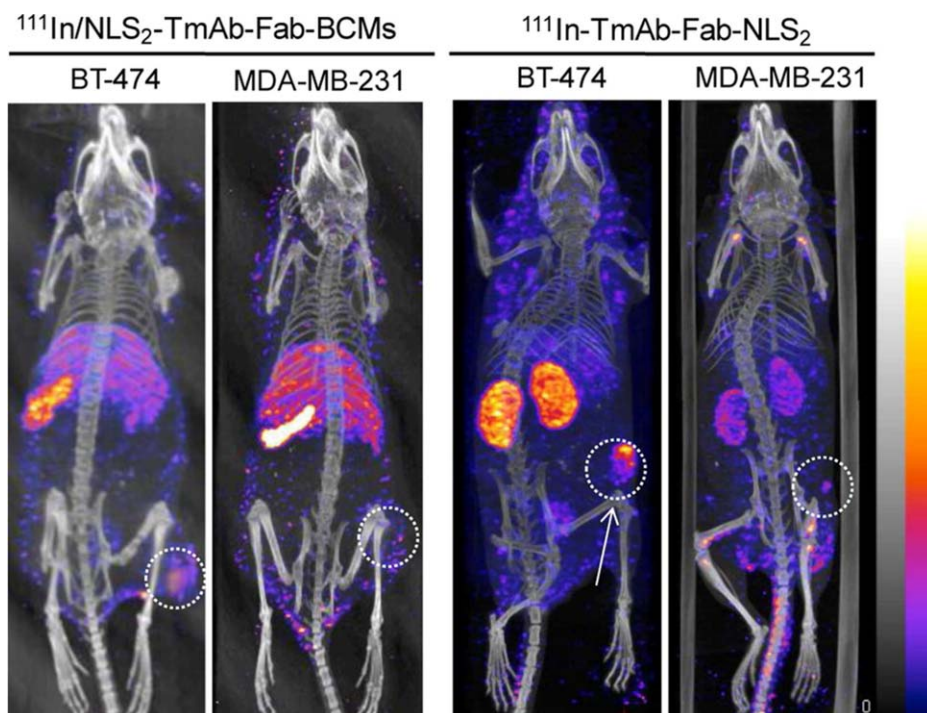


**Figure 2.** Micro-single-photon emission tomography–computing tomography images of athymic mice bearing BT-474 (HER2–overexpressing) or MDA–MB-231 tumors (HER2–low-expressing). An enhanced accumulation, most likely due to active targeting, of the targeted TmAb–Fab–PEG–*b*-PCL BCMS was observed on the HER2–overexpressing BT-474 tumors (white arrow). Reproduced with permission from ref. 82. Copyright 2013 American Chemical Society. [Color figure can be viewed in the online issue, which is available at [wileyonlinelibrary.com](http://wileyonlinelibrary.com).]

enhancement takes place.<sup>61</sup> Another particular aspect that affects micellar stabilization is the effect of the micellar specific surface area.<sup>67</sup> The micellar stability is further dependent on the nature of the core-forming polymer, with (semi)crystalline micelle cores being more stable than amorphous ones and enabling lower rates of drug diffusion.<sup>68</sup> BCMS with a hydrophobic block with a glass-transition temperature exceeding 37°C possess cores stabilized by the restricted motion of glassy segments; this affords a greater kinetic stability of the micelles upon dilution. However, these frozen cores also decrease their solubilization capacity, as observed when BCMS are compared with polystyrene (PS) and PSO cores of similar block lengths.<sup>69</sup> Finally, the crosslinking of the micellar corona–core is yet another promising approach for improving the stability of micelles according to the pioneering work by Wooley’s group.<sup>53</sup> Crosslinking strategies rely on the presence of functional groups within the domains of either hydrophilic and/or hydrophobic blocks of a copolymeric chain; this results in crosslinkages at the hydrophilic shell, hydrophobic core, or core–shell interface of the micelle via chemical crosslinks, photocrosslinks, or polymerization after the micelle formation via self-assembly in aqueous solution.<sup>70</sup> The location of this reactive sites has a great influence on the physicochemical properties of the resulting crosslinked micelles. Crosslinking reactions might be spontaneous through the simple use of an external physical or chemical change experienced in the surroundings of the BCMS (e.g., temperature, pH, ionic strength). Alternatively, additional reactive moieties can be either covalently linked (with crosslinking agents which do not

remain within the polymeric structure, e.g., carbodiimides) or, through the simple introduction of small difunctional crosslinkable pendants or short polymeric chains through labile bonds, capable of being assembled–disassembled by the effect of an external stimulus, for example, light irradiation (see later discussion). For more detailed information about crosslinkable micelles, refer to the excellent reviews that have been published elsewhere.<sup>70–72</sup>

#### Micellar Targeting

The hydrophilic shell plays a key role in providing protection to the drug cargo molecules by preventing its degradation at off-target sites; this contributes to longer blood circulation times and better stability. To do that, a biocompatible polymer corona serves to suppress and minimize nonspecific interactions with biological components; this includes opsonization by plasma proteins, scavenging by the mononuclear phagocytic system in the liver, and filtration of interendothelial cells in the spleen. This stealth property is essential for ensuring the accumulation of drugs at the site of action via the enhanced permeation and retention (EPR) effect, a process also known as *passive targeting*. Generally, free drug molecules can easily pass through the vascular endothelium and indiscriminately distribute themselves into all tissues, but the drug can also return relatively rapidly to the blood stream and be eliminated from the body. The short residence time at the active site and the exposition of nontarget tissues to the drug lead to limited therapeutic efficacy and notable side effects.<sup>73</sup> The stealthiness and nanosize of BCMS, which are similar to that of viruses, lipoproteins, and other biological

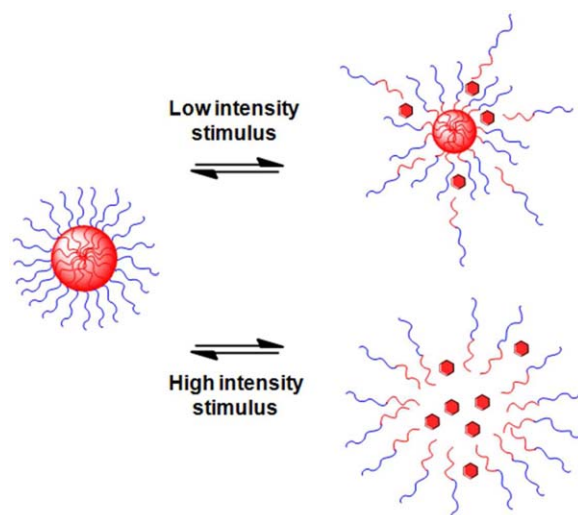


**Figure 3.** BCMs with a controllable response depending on the intensity of the applied stimulus. [Color figure can be viewed in the online issue, which is available at [wileyonlinelibrary.com](http://wileyonlinelibrary.com).]

systems of transport, take benefit, for example, of the leaky vasculature of tumors, inflamed tissues, and infarcted areas. The vascular abnormalities, due to newly formed vessels with poorly aligned endothelial cells, which are common to almost all tumors, result in endothelial pores that can be as large as 100–1000 nm; this facilitates the entrance of the BCMs. Additionally, the lymphatic drainage is defective, and consequently, the tumors present erratic fluid and molecular transport dynamics.<sup>74</sup> Overall, these pathological characteristics lead to hyperpermeability and the subsequent accumulation of drug-loaded nanosized vehicles. For these reasons, BCMs with dense hydrophilic silent surfaces, such as PEG blocks, and with sizes between 10 and 100 nm, which are sufficiently large enough to prevent renal excretion (>50 kDa) but yet small enough (<200 nm) to bypass interendothelial cell slits in the spleen, may exhibit improved accumulation in tumor tissues.<sup>75</sup> Small silent micelles have been shown to accumulate in tumor tissue at concentrations 10–30 times (even up to 2000 times) higher than their concentration in plasma 24 h after intravenous injection and frequently at levels more than 10 times higher than that in normal tissue.<sup>76</sup>

Nevertheless, in some situations in which passive targeting is not sufficient for discriminating between healthy and diseased cells or tissues, the targeting ability might be notably improved if the micelle is decorated with ligands that bind specifically to receptors overexpressed in the target cells.<sup>77</sup> These ligands can form part of the initial block copolymer or be conjugated to the preformed BCMs. Molecules of quite a different nature can be used as targeting ligands. Small molecules, such as folic acid and biotin, recognize with a great specificity the overexpressed receptors at cancer cells.<sup>78</sup> Peptides and aptamers have been also proven successful for micelle targeting.<sup>79</sup> As such, the tripeptide Arg–Gly–Asp (RGD) can bind to the  $\alpha_v\beta_3$  integrin receptor, which is largely expressed at the surface of malignant cells and in tumor-proliferating neovascular endothelial cells.<sup>80</sup> Carbohydrates bind specifically to the asialoglycoprotein receptors com-

monly found in liver cells.<sup>81</sup> Micelles with surface-attached antibodies, known as *immunomicelles*, provide a wide variety of targets and specificity of interactions while retaining the ability of antibodies to specifically interact with their antigens as, for example, in the case of radiolabeled trastuzumab (TmAb)-decorated [Fab fraction (TmAb–Fab)]–PEG–PCL micelles, which show an enhanced accumulation and site-specific localization in mice bearing subcutaneous human epidermal growth factor receptor 2 (HER2) positive BT-474 tumors, as observed by micro-single-photon emission tomography–computing tomography (Figure 2).<sup>82</sup> Magnetic targeting is another strategy that has been used to guide micellar systems to diseased organs and tissues. This targeting modality relies on the placement of a magnet near the region where the accumulation of micelles is desired. Certainly, BCMs must be loaded with or be functionalized with magnetic responsive agents, for example, with superparamagnetic iron oxide nanoparticles (SPIONs).<sup>83</sup> Readers interested in ligand and magnetic-active targeting should refer to the comprehensive reviews published elsewhere.<sup>77,78,84,85</sup>

### Drug Release: Stimuli-Responsive BCMs

The first generation of BCMs were designed to gradually release the payload over time through the equilibrium nature between free and encapsulated drugs, their dilution below the cmc, the hydrolytic degradation of drug-loading blocks in the body, or nonspecific exchange reactions with biological components. In these cases, the time-dependent drug-release profile is critical for the biological performance of BCMs, as drug release should be concurrent with micelle accumulation at the target sites. To establish such a correlation, drug release should be activated to attain high concentrations of drug at the diseased area.

On the basis of the former idea, the second generation of BCMs were further customized with the ability to release their payload under certain variables of the site where release should occur. Those variables could be the physicochemical peculiarities of the body site (internal stimuli) as pH<sup>86,87</sup> and temperature

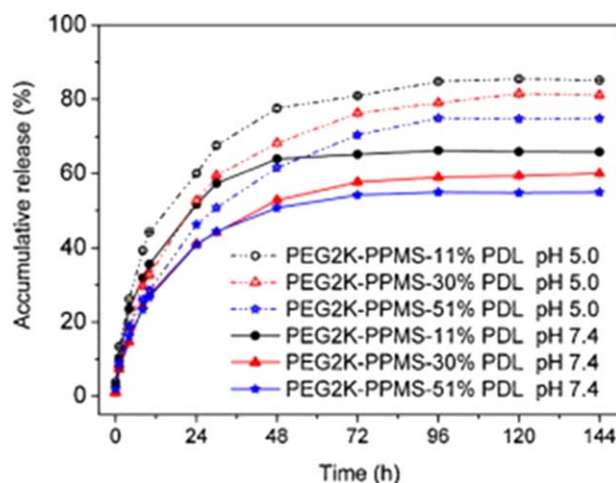


**Figure 4.** Release of PTX from PEG–PPMS BCMs. At a mildly acidic pH of 5 (lysosomal), enhanced release was observed in comparison with the release at pH 7.4 (blood and healthy tissues). Reproduced with permission from ref. 108. Copyright 2014 Elsevier. [Color figure can be viewed in the online issue, which is available at [wileyonlinelibrary.com](http://wileyonlinelibrary.com).]

changes,<sup>88,89</sup> the presence of counterions and enzymes,<sup>47,90</sup> or redox potential;<sup>91,92</sup> alternatively, the changes could be externally induced (external stimuli) through the application of, for example, light,<sup>93,94</sup> ultrasound,<sup>95</sup> or magnetic fields.<sup>96</sup> Stimuli-responsive micelles can be prepared with block copolymers that can undergo changes in their solvent affinity, conformation, or bonds under a given stimulus that changes their equilibrium association state<sup>53</sup> or by the incorporation of sensitive external elements (e.g., gold or magnetite nanoparticles) that can recognize the stimulus; this leads to local perturbations that trigger micelle disassembly.<sup>97</sup> Readers interested in materials useful for preparing responsive nanocarriers are referred to recent reviews on the field.<sup>98–101</sup> Ideally, stimuli-responsive micelles to be considered as smart carriers should disintegrate or destabilize in a number proportional to the intensity of the stimulus, and consequently, the drug release rate could be tuned. If the stimulus stops, the micelles could re-form, and the release could be interrupted (Figure 3). In the following sections, we give a brief description of the preparation and features of different types of stimuli-responsive BCMS.

**pH-Responsive BCMS.** The stimulus for many responsive BCMS can be the pH gradients frequently found within the human body. For instance, along the gastrointestinal tract, the pH varies from 1.00 to 3.00 in the stomach to 4.80–8.20 in the upper gut and to 7.00–7.50 in the colon. Inside cells, pHs from 7.4 in the cytosol, 6.40 in the Golgi apparatus, 5.5–6.0 in the endosome, and 4.5–5.0 in lysosomes are found.<sup>102</sup> The incorporation of pH responsiveness is an interesting tool for the selective release of drugs in pathologies that are characterized by acidosis (pH < 7.4); these include ischemia, infection, inflammation, and tumoral processes with a decreased extracellular pH.<sup>103</sup> Oppositely, the wounds commonly show an increase in pH from 4 to 6 (normal skin) up to values that can be as high as 8.9.<sup>104</sup>

Often, pH-sensitive block polymers bear weak acid or base groups. The group-containing block shows a hydrophobic behavior when these groups are not ionized (below their  $pK_a$ ), so they are responsible for copolymer self-assembly. Micelles are stable as long as the pH of the medium does not induce the ionization of the chemical groups. Upon ionization, an increase in the polarity and electrostatic repulsions among the ionizable blocks results in the disintegration of micelles. The triggering pH depends on the  $pK_a$  of the chemical groups and, thus, can be tuned by means of the copolymer composition.<sup>105</sup> Amphiphilic copolymers with amino groups on one of their blocks, such as poly( $\beta$ -amino esters)<sup>106</sup> or polyamines,<sup>107</sup> have been demonstrated to demicellize and release their cargo under acidic pH conditions by the protonation of amino groups and subsequent electrostatic repulsions of the formerly neutral blocks. For example, Zhang *et al.*<sup>108</sup> recently developed a pH-sensitive micellar nanocarrier for (docetaxel DTX) formed from pegylated poly (amine-*co*-ester) blocks (i.e.,  $\omega$ -pentadecalactone, *N*-dimethyl diethanolamine, and diethyl sebacate), PEG-*b*-poly( $\omega$ -pentadecalactone-*co*-*N*-dimethyl diethanolamine-*co*-sebacate) (PPMS), which showed a pH-dependent assembly–disassembly behavior that was attributable to the protonation–deprotonation of amino groups in the PPMS cores. The release of the antineoplastic DTX was notably accelerated by the modification of the

pH of the suspending medium from 7.4 to 5.0 (Figure 4).<sup>108</sup> Following the same underlying mechanism, block copolymers bearing a polypeptide block in their structure, such as PLys, poly(L-glutamic acid), or poly(benzyl glutamate), also offer an alternative for achieving a controlled pH–micellar disruption and achieved a controlled cargo release.<sup>109–112</sup>

An alternative approach for obtaining pH-responsive BCMS is the use of copolymers with functional groups–bonds susceptible to degradation at mildly acidic pHs. Different acid labile bonds, such as orthoesters, hydrazones, and acetals, have been positioned either in the main chain, at the side chain, or at the terminal of the core-forming block. For example, BCMS bearing orthoester pendants formed by PEG-*b*-poly(2-ethoxytetrahydrofuran-2-yloxyethyl methacrylate) chains underwent rapid degradation at a mildly acidic pH, and the concomitant fast release of a model hydrophobic molecule, Nile Red, was attained.<sup>87</sup> Also, the anticancer drug doxorubicin (DOX) was covalently conjugated into aspartate side chains of a PEG–PAsp copolymer through a hydrazone bond to form a pH-sensitive BCM. The selective release of the cargo at endosomal pH (< 6.5) was found, and suppressed tumor growth in mice with an enhanced therapeutic efficacy and decreased systemic toxicity compared to free DOX was reported.<sup>8</sup>

Moreover, pH-responsive polymeric micelles have been particularly adequate as nonviral vectors of DNA and small interfering RNA (siRNA).<sup>5</sup> The nucleotides interact with the amino groups of the copolymer and form a complex that is included inside the micelle (micelleplex); this provides protection against enzymatic attack.<sup>113</sup> For instance, Kim *et al.*<sup>22</sup> developed BCMS with a hydrophilic PEG corona, an intermediate cationic PLys shell, and a core formed by poly{*N*-[*N*-(2-aminoethyl)-2-aminoethyl] aspartamide} bearing hydrophobic dimethoxynitrobenzyl ester moieties for the encapsulation and cellular delivery of siRNA. Here, the intermediated PLys shell acted as a reservoir for siRNA, efficiently protecting it from external conditions while ensuring its release once inside acidic cellular compartments (endosomes and lysosomes), as observed by confocal laser microscopy and Förster resonance electron transfer techniques performed in luciferase-modified HeLa cells.

**Thermoresponsive BCMS.** Several pathological conditions (e.g., inflammation, infarction, tumors) evolve with local increases in temperature. Moreover, site-specific temperature increments can be achieved by the application of an external heat source on the skin or can be remotely induced through various types of radiation that can be absorbed by some components of the nanocarrier that transform it into heat. Commonly, temperature-sensitive polymeric chains are hydrophilic below their lower critical solution temperature (LCST). When the temperature is above LCST, the polymer chain becomes hydrophobic, and its conformation changes from an expanded (soluble) to a globular (insoluble) state. The most common example of this type of polymers is PNIPAAm, which, when used as the hydrophilic block, leads to micelles at temperatures below LCST (ca. 32°C).<sup>91</sup> Above LCST, the micelle destabilizes, and the loaded drug can be released. In a representative example of thermoresponsive BCMS, Luo *et al.*<sup>114</sup> synthesized an amphiphilic block copolymer with a brush-shaped



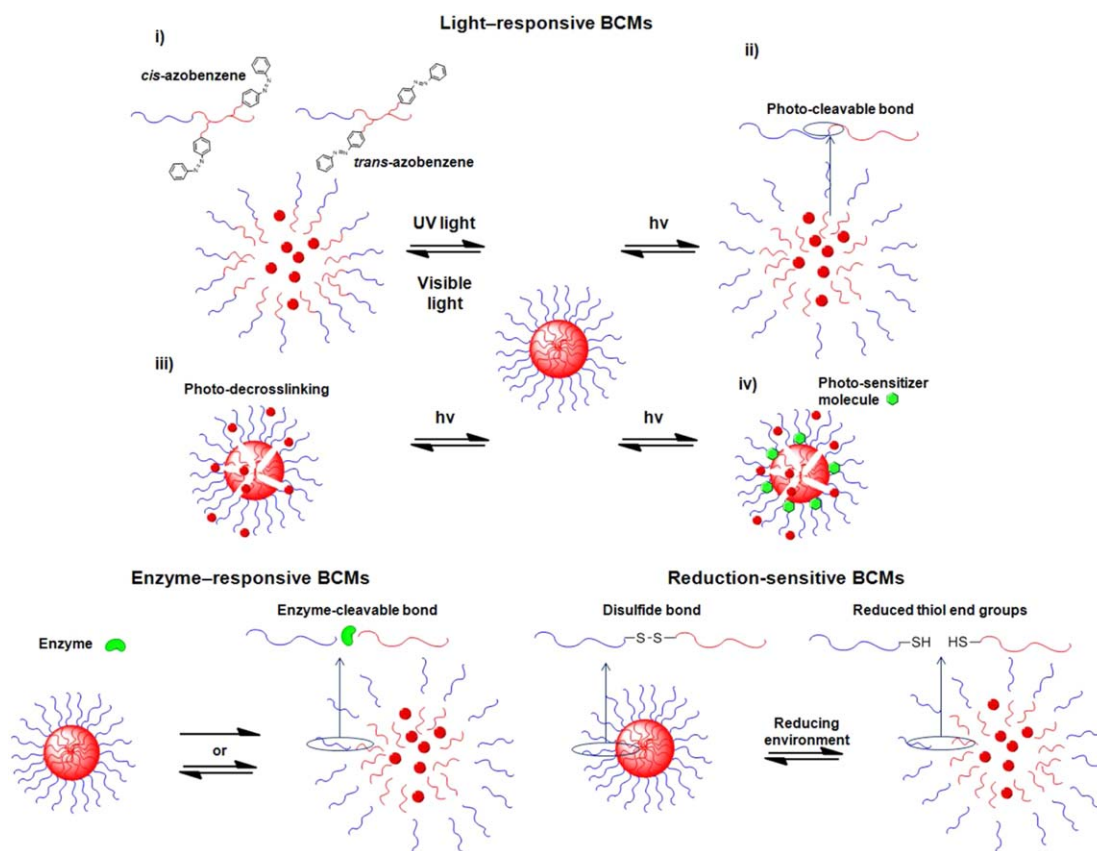


**Figure 5.** Light-responsive BCMs. (i) Photoisomerization-based systems change the aggregation state upon stereochemistry changes of certain molecules within the hydrophobic block. (ii) Photodegradable systems are built from copolymers bearing light-cleavable bonds between hydrophobic and hydrophilic blocks. (iii) Photocrosslinking–decrosslinking systems include in their structure moieties sensitive to subtle changes in light-triggered crosslinking–decrosslinking reactions. (iv) Photosensitization-based systems include sensitizing molecules, which generate highly oxidizing species (e.g., singlet oxygen) upon illumination, which subsequently disrupt the micelle. Enzyme-responsive BCMs may be light-switchable (reversible) or disrupted (irreversible) after the action of a specific enzyme on certain block copolymer bonds. Reduction-sensitive BCMs generally include reducible bonds (e.g., disulfide bonds) in their polymeric components. [Color figure can be viewed in the online issue, which is available at [wileyonlinelibrary.com](http://wileyonlinelibrary.com).]

architecture composed of a polyacrylate (PA)–PEG–PA backbone and thermosensitive PNIPAAm short side chains at both ends of the PEG chain, [PNIPAAm-*g*-(PA–PEG–PA)-*g*-PNIPAAm]. The micelles obtained featured a core–shell–corona structure with a hydrophobic PA inner core, a thermoresponsive PNIPAAm shell, and a hydrophilic PEG corona; these provided the system with the biocompatibility of PEG and the thermosensitive behavior of PNIPAAm. DOX encapsulation and release was also evaluated for a series of BCMs made from PNIPAAm and hydrophobic poly(*N*-acryloyl-2-pyrrolidone) blocks of different lengths.<sup>115</sup> Although the drug release was almost negligible at 20°C, a clear enhancement was observed when the temperature rose to 37°C, with slower diffusion rates noted for micelles with the most hydrophobic cores. Other thermosensitive micelles have been designed with blocks other than PNIPAAm. For instance, micelles based on poly(*N*-vinyl caprolactam)–PEG–folic acid with an LCST of 33°C were prepared and showed a slow sustained release profile of entrapped 5-fluoracil up to 30 h.<sup>116</sup>

**Light-Responsive BCMs.** Light—UV, visible, or IR—can be used as an external stimulus for controlled micelle disassembly–reassembly. Particularly, UV and visible light are not able to

penetrate deeply into tissues because of absorption by skin, and in particular, UV light is toxic to cells and tissues. Near-infrared (NIR) light penetrates deeper in the body (up to several centimeters) because hemoglobin (the principal absorber of visible light), water, and lipids (principal absorbers of IR light) have low absorption in the NIR region (650–900 nm), so NIR light can be directly used to trigger drug release from micelles. This can be done via four different physicochemical mechanisms (Figure 5):<sup>39</sup>

1. Photoisomerization, which is related to a conformational change around a bond that is restricted in rotation. Usually, this process involves a trans-to-cis isomerization of a chemical group or block of a copolymer upon irradiation or the generation of charged species; this involves a change in the hydrophilic–hydrophobic balance of the photoexcitable molecules. For example, Bossiere *et al.*<sup>117</sup> reported flowerlike micelles containing hydrophobically modified PNIPAAm with multiple azobenzene segments incorporated into the main chain. The micelles responded to both UV and visible light by undergoing reversible trans–cis isomerization and remained well dispersed even above the LCST of PNIPAAm chains; this was caused by the



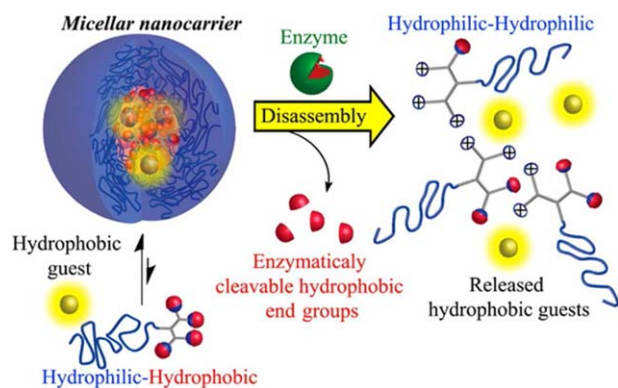


**Figure 6.** Scheme of a PEG–dendron micelle sensitive to subtle changes in degradation by penicillin G amidase and subsequent cargo release. Reproduced with permission from ref. 132. Copyright 2014 American Chemical Society. [Color figure can be viewed in the online issue, which is available at [wileyonlinelibrary.com](http://wileyonlinelibrary.com).]

aggregation of azobenzene moieties. Recently, spyropyranyl-initiated hyperbranched polyglycerol micelles were reported; this responded to UV–visible light and could dissociate because of the conversion of the hydrophobic chromophore (spyropyranyl SP) to zwitterionic and hydrophilic merocyanine.<sup>118</sup>

2. Photodegradation, which enables cargo release through the rupture of labile bonds in the copolymer backbone or the junctions between blocks and triggers micellar disruption. The most used photocleavable junctions are *o*-nitrobenzyl based moieties,<sup>119</sup> truxilic acid derivatives,<sup>120</sup> and inclusion complexes of azobenzenes and cyclodextrins (CDs), the latter being of remarkable interest because of its reversibility, as demonstrated by the assembly and disassembly of light-responsive nanotubes formed on the basis of orthogonal host–guest interaction between PCL– $\alpha$ CD and PAA–tAzobenzene block copolymers.<sup>121</sup>
3. Photocrosslinking and photodecrosslinking, in which light modifies the crosslinking density of block copolymers. As a consequence, their conformation results in the formation of pores in the micelles. For example, Zhao *et al.*<sup>122</sup> designed a random copolymer with PEO and a hydrophobic block of 4-methyl-(7-methacryloyl)oxy ethyloxy coumarin and methyl methacrylate. In aqueous media, upon UV irradiation, the dimerization degree of photoresponsive groups can be varied between 20 and 80%; this depends on the light wavelength and, hence, alters the crosslinking density of the micellar core.
4. Photosensitization-induced oxidation, in which the irradiation of a sensitizer molecule incorporated into the micelle may lead to strong oxidizing species (e.g., reactive oxygen species) that disrupt the nanocarrier. Alternatively, pathophysiologic oxidative stress conditions might also drive micellar disassembly. For example, the BCMs of poly(propylene sulfide)-*b*-poly(*N,N*-dimethyl acrylamide) loaded with Nile Red as a model drug showed an oxidation-induced release of their cargo in the presence of three different oxidizing agents: H<sub>2</sub>O<sub>2</sub>, 3-morpholinopyridone, and peroxyacetyl nitrate.<sup>123</sup>

**Ultrasound-Responsive BCMs.** Ultrasound can be exploited to induce the mechanical disruption of the BCMs; this is another

alternative for triggering drug release in a controlled manner. Ultrasound refers to the application of pressure waves above a frequency of 20 kHz to spatially and temporally control drug release.<sup>124</sup> Pluronic micelles have been investigated extensively for the ultrasound-triggered delivery of both drugs and nucleic acids.<sup>125,126</sup> The amount of drug release can be modulated through the control of the ultrasound frequency, power density, pulse length, and interpulse intervals.<sup>124</sup> Although low-frequency ultrasound (20–100 kHz) can penetrate deeper into body tissues than high-frequency ultrasound (1–3 MHz), it cannot be focused as well.<sup>127</sup> *In vitro*, ultrasound can perturb the micelle structure and cause the release of therapeutic payloads triggered by oscillating or cavitating bubbles. *In vivo*, this mechanical effect of ultrasound may also be accompanied by local hyperthermia, which can lead to increased micelle extravasation and accumulation in target tissues.<sup>125</sup> Ideally, the ultrasound should be applied at the moment of peak accumulation of micelles at the disease site. *In vitro* and *in vivo* studies revealed an important antitumoral effectiveness, probably promoted by cell membrane perturbation and subsequent pore formation (sonoporation) by ultrasound waves; this enhances the intracellular uptake of nanocarriers by tumor cells.<sup>125</sup> For example, ultrasound-sensitive, PTX-loaded BCMs of methoxy PEG and poly(D,L-lactide) (MePEG-*b*-PDLLA) resulted in increased PTX accumulation and subsequently enhanced cytotoxicity in both drug-sensitive and drug-resistant (*P*-glycoprotein expressing) cell lines.<sup>128</sup>

**Enzyme-Responsive BCMs.** Enzymes in the body are useful both for fixing together polymer chains, which leads to the formation of self-assembled or covalently bonded networks, or for breaking certain bonds, which causes disassembly or network rupture.<sup>98</sup> As a result, enzymes, either in healthy bodies or their hypoexpressed–hyperexpressed states, which lead to a range of disease states, could be exploited to directly act on sensitive drug carriers and trigger cargo release in localized cells or tissues.

An enzyme-responsive BCM requires at least an enzyme-sensitive component, which is a substrate of the enzyme (e.g., enzyme-sensitive moieties inside the polymeric chains or BCM surfaces modified with peptides or oligonucleotides undergoing physical changes under enzymatic transformations),<sup>129</sup> whereas the drug can be chemically or physically entrapped in the nanocarrier and be released upon the catalytic action of the enzyme. Changes in the properties of the enzyme-responsive BCMs can be triggered either by (1) alterations of covalent bonds or (2) modifications in the balance of combined weak bonds (e.g., electrostatic interactions, van der Waals interactions,  $\pi$ – $\pi$  interactions) by the action of proteases, kinases, phosphatases, glycosidases, and oxidoreductases.<sup>130</sup> To be effective, enzyme-responsive BCMs have to be able to reach the enzyme and expose sensitive groups to it. This is particularly critical when the enzymatic activity is associated with a particular tissue or when the enzyme is found at high concentrations at a certain site. Thus, detailed knowledge about both the extracellular and intracellular barriers is required to attain successful enzyme-responsive release. Enzyme-responsive micelles can be categorized into two

classes according to their physical response upon catalytic action of the enzyme:

1. Disruptive enzyme-responsive BCMs, which are micelles that lose the original structure of the unimers after the enzymatic reaction by selectively cleaving a bond; this divides the molecular structure of the polymeric chains into two or more parts that are not able to self-assemble any more (Figure 5), as done by Zhu *et al.*,<sup>131</sup> who developed BCMs bearing a matrix metalloproteinase (MMP)-sensitive peptide for the tumor-specific delivery of drugs and siRNA in response to overexpressed MMPs. Recently, Harnoy *et al.*<sup>132</sup> prepared micelles based on hydrophilic PEG and hydrophobic enzyme-responsive dendrons (PEG-dendron), whose disassembly was activated through enzymatic degradation with penicillin G amidase (Figure 6).
2. Switchable micelles, in which the disassembly process occurs without disruption of the original structure of the polymeric chains. Available examples are mainly based on the catalytic activity of phosphatases. For example, the cationic hydrophilic block of a PEG-poly(L-Lys HCl) copolymer can interact with ATP to incorporate the hydrophobic functionality of adenosine, turn the polymer amphiphilic, and lead to self-assembled micelles. Upon enzymatic dephosphorylation, ATP is degraded to adenosine and single-charged phosphate groups, which are not able to bind the poly(L-Lys HCl) block and, thus, the micelles fall apart.<sup>133</sup>

**Reduction-Sensitive BCMs.** The fast and reversible thiol-disulfide exchange reactions play an important role in maintaining the proper biological functions of living cells; these include the stabilization of protein structures, enzymatic activity, and redox cycles. Glutathione tripeptide [ $\gamma$ -glutamyl-cysteinyl-glycine (GSH)]/glutathione disulfide is the major redox couple in animal cells. Blood, an extracellular environment, and cell surfaces possess a low concentration of GSH (2–20  $\mu$ M). Oppositely, an intracellular concentration of GSH is 0.5–10 mM; this is reduced by nicotinamide adenine dinucleotide phosphate NADPH and glutathione reductase and maintains a highly reducing environment.<sup>134</sup> Endosomal and lysosomal compartments are also rich in reducing agents.<sup>135</sup> Moreover, tumor tissues contain fourfold higher concentrations of GSH than normal tissues.<sup>136</sup> These differences in the GSH concentration have prompted the development of BCMs, in which disulfide bonds in the polymer main chain, at the polymer side chain, or in the crosslinker can provide stability while they circulate in the blood stream, but once inside healthy cells or in the surroundings of tumor tissues, micelles can disintegrate as the disulfide bonds break in thiol groups. This leads to the controlled and efficient release of drug molecules in the cytoplasm and/or cell nuclei.<sup>137,138</sup> Three different approaches have been followed so far to obtain GSH-responsive micelles:

1. Shell-sheddable BCMs. PEG-SS-PCL<sup>139</sup> or PEG-SS-poly( $\gamma$ -benzyl-L-glutamate) (where SS denotes a disulfide bond) form stable micelles in aqueous media, but inside cells, the PEG shells detach because of the reductive cleavage of the intermediate disulfide bonds; this releases the cargo at much

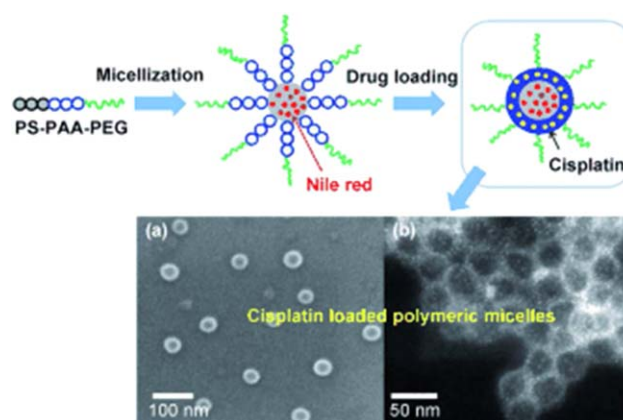


**Figure 7.** Multifunctional polymeric micelles coloaded with the imaging agent Nile Red and the anticancer drug cisplatin: (a) scanning electron microscopy and (b) transmission electron microscopy images of the cisplatin-loaded polymeric micelles. Reproduced with permission from ref. 149. Copyright 2013 Wiley. [Color figure can be viewed in the online issue, which is available at wileyonlinelibrary.com.]

faster rates than similarly prepared reduction-insensitive micelles (Figure 5).

2. Reduction-sensitive core BCMs. Amphiphilic copolymers containing disulfide bonds in the hydrophobic segments, such as PEO-*b*-poly[*N*-methacryloyl-*N'*-(*t*-butyl oxycarbonyl) cystamine],<sup>140</sup> can be broken when the GSH concentration increases. This leads to micelle disintegration.
3. Reduction-sensitive crosslinked BCMs. Once the micelles are formed, the copolymers can be crosslinked with redox-responsive labile bonds to enhance the *in vivo* stability while ensuring intracellular cargo release. In this manner, shell-crosslinked micelles have also been obtained through the self-assembly of PEG-poly(L-Lys)-poly(L-phenyl alanine) triblock copolymers followed by the crosslinking of the poly(L-lys) block with 3,3'-dithiobis(sulfosuccinimidyl propionate).<sup>141</sup>

Other alternative approaches for the design of reduction-sensitive BCMs is the exploitation of gradients of oxygen tension within tumors, as demonstrated by Perche *et al.*,<sup>142</sup> who developed hypoxia-activated PEG-PEI-1,2-dioleyl-*sn*-glycero-3-phosphoethanol amine micellar nanocarriers for siRNA encapsulation to achieve the downregulation of a model gene (GFP) *in vitro* and *in vivo* with azobenzene groups linked to both PEG and PEI-1,2-dioleyl-*sn*-glycero-3-phosphoethanol amine blocks as hypoxia-responsive, bioreductive linkers.

**Multiresponsive BCMs.** Materials that respond to several stimuli independently or in a synergistic way are particularly useful for the design of multiresponsive micelles.<sup>143</sup> The advantage of micelles that recognize changes in two or more variables is that they can more precisely regulate the site and the rate of the release process because most pathological processes cause changes in several physicochemical parameters simultaneously. In that way, the risk of drug release in a nontarget tissue is minimized. Probably, star-shaped PEO-PPO block copolymers are one of the most extensively investigated multiresponsive micelle-forming copolymers because of their commercial availability in different molecular weights and their EO-PO ratios.

Their ethylenediamine central moiety (and two tertiary) amines confers molecule responsiveness to pH and enables the chemical modification of the core; the presence of PPO and PEO blocks in their molecular structure provides them with temperature-dependent self-assembling properties.<sup>13,144</sup> Another example of multiresponsive micelles are those formed by PNIPAAm-SS-poly(tetrahydroxyran-protected 2-hydroxyethyl methacrylate) block copolymer chains [PNIPAAm-SS-poly(tetrahydroxyran-HEMA)], which provide the fine tuning of the release kinetics of hydrophobic cargos in response to temperature, pH, and redox potential changes.<sup>145</sup> Although the pH and redox potential separately cause the slow or incomplete release of Nile Red over long periods of times, the combination of such stimuli results in accelerated and profuse cargo release.

Multistimuli responsiveness can also be exploited to control the release of several drugs in response to different internal or external signals.<sup>146</sup> For example, Chen *et al.* developed a dual pH-reduction activated micelle composed of the pH-sensitive block poly[(2-diisopropyl amino)ethyl methacrylate] (PDPA), a reduction-sensitive poly{N-[2,2'-dithiobis(ethylamine)] aspartamide} [PAsp(AED)] block, and hydrophilic PEG [PEG-*b*-PDPA-*b*-PAsp(AED)]. Micelles formed by this triblock copolymer were able to encapsulate the anticancer drug DOX and therapeutic siRNA targeting the antiapoptosis gene BCL-2. The pH-sensitive core formed by PDPA shielded DOX from contact with the external milieu, whereas the intermediate reduction-sensitive layer formed by PAsp(AED) protected siRNA from degradation by nucleases. Once inside the lysosomal compartments, both therapeutic agents were released, displaying a synergistic antitumor effect *in vitro* and *in vivo* because of the sensitization of the DOX chemotherapy by BCL-2 knockdown.<sup>147</sup>

**Multifunctional BCMS.** Thanks to their special architecture, BCMS may be easily loaded or tagged with multiple moieties; this enables the simultaneous combination of at least two different features regarding triggered therapeutic drug release, imaging, sensing, and targeting in the same nanostructure.<sup>148</sup> For example, BCMS with truly segregated core domains could facilitate the encapsulation of incompatible hydrophobic drugs, fluorescent molecules, small nanoparticles [e.g., gold nanoparticles (Au NPs), SPIONs, quantum dots (QDs)], or bioactive molecules within a single micelle.<sup>149–151</sup> Moreover, BCMS with different functional groups in their exposed hydrophilic blocks can be decorated with therapeutic and contrast agents and targeting ligands to achieve multifunctionality.<sup>152–154</sup>

Bifunctional approaches have been largely studied during past years. The combination of imaging agents and triggered release enables micelle tracking in the body and on-command triggered release once the micelles reach their target area, whereas the combination of active targeting and triggered release results in more efficient drug delivery.<sup>155</sup> For instance, core-shell-corona micelles seem to be optimal structures for building multifunctional systems because of the multicompartiment inner phase and the stabilization and ease of functionalization provided by a hydrophilic outer layer, ideally PEG. This idea led to Bastakoti *et al.*<sup>149</sup> to design an asymmetric triblock copolymer (PS-*b*-PAA-*b*-PEG) for the development of multifunctional BCMS with the fluorescent imaging dye Nile Red inside

the frozen PS core, the anticancer drug cisplatin within a pH-sensitive PAA shell, and a hydrophilic neutral PEG corona (Figure 7). A selective mineralization of calcium phosphate on the PAA shell enabled the enhancement of the fluorescence intensity of the dye by protecting it from the polar external environment and preventing the rapid release of the drug by acting as a pH-responsive diffusion barrier. In another study, PLGA-PEG BCMS were reported for the combined delivery of DOX and PTX. A cell-penetrating enhancing moiety (TAT) and a targeting ligand (folate) were used to modify PLGA-PEG to achieve an enhanced therapeutic effect for the drug combination versus the single drugs. Dual-drug-loaded micelles modified with both ligands were observed to exhibit a significantly lower IC<sub>50</sub> values in KB cells (mouth epidermal carcinoma cells) compared to single-drug-loaded micelles. Although a synergistic effect was observed with both methods (the codelivery of two single-drug-loaded micelles and dual-drug-loaded micelles), it was hypothesized that the drug ration would be better maintained in the dual-loaded bifunctional formulation *in vivo* compared to the codelivery of dual-targeted, single-drug-loaded micelles.<sup>156</sup>

On the other hand, trimodal (targeting, therapy, and imaging) or even multimodal (a combination of several types of targeting, therapy, and imaging capabilities at the same time) micelles have been less developed. However, recent studies have demonstrated the ability of polymeric micelles to hold the same nanostructure with all of their required capabilities. For instance, Hoang *et al.*<sup>82</sup> developed radiolabeled <sup>111</sup>In-PEG-PCL BCMS functionalized with the Fab fragment of the monoclonal antibody TmAb (herceptin, TmAb-Fab) and nuclear localization signal (NLS) peptides. In this micellar system, the radionuclide <sup>111</sup>In acts as a therapeutic and contrast agent, whereas TmAb-Fab acts as a targeting ligand to tumoral cells, and NLS peptides act as a specific ligand for nuclear inclusion of the nanocarrier. The cellular uptake of the radiotherapeutic BCMS was observed to depend on HER2 surface cell expression, and a significant depletion of survival fraction was observed on BC cells with a high HER2 receptor density. Approximately 43% of the internalized micellar population was successfully transported to the nucleus of the cells thanks to the NLS domains in BCMS. In addition, *in vivo* studies showed the effective cell association and uptake of the actively targeted <sup>111</sup>In/NLS-PEG-PCL-TmAb-Fab micelles because of HER2 and nuclear targeting in BT-474 tumors. Similarly, Guo *et al.*<sup>157</sup> developed trimodal unimolecular micelles for cancer-cell targeting, imaging, and therapy from the dendritic amphiphilic block copolymer polyamidoamine-PLA-PEG conjugated with the anti-CD105 monoclonal antibody (TRC105) and 1,4,7-triazacyclononane-*N,N'*-triacetic acid (a macrocyclic chelator for <sup>64</sup>Cu). Here, DOX was incorporated into the hydrophobic core of the unimolecular micelles and released when the pH decreased as a consequence of the deformation of the inner micellar core. In 4T1 murine breast tumor-bearing mice, the <sup>64</sup>Cu-labeled targeted micelles exhibited a much higher level of tumor accumulation than the <sup>64</sup>Cu-labeled nontargeted micelles measured by serial noninvasive positron emission tomography imaging and confirmed by biodistribution studies.

The incorporation of inorganic nanoparticles, such as SPIONs, QDs, or Au NPs, within polymeric micelles has also allowed to



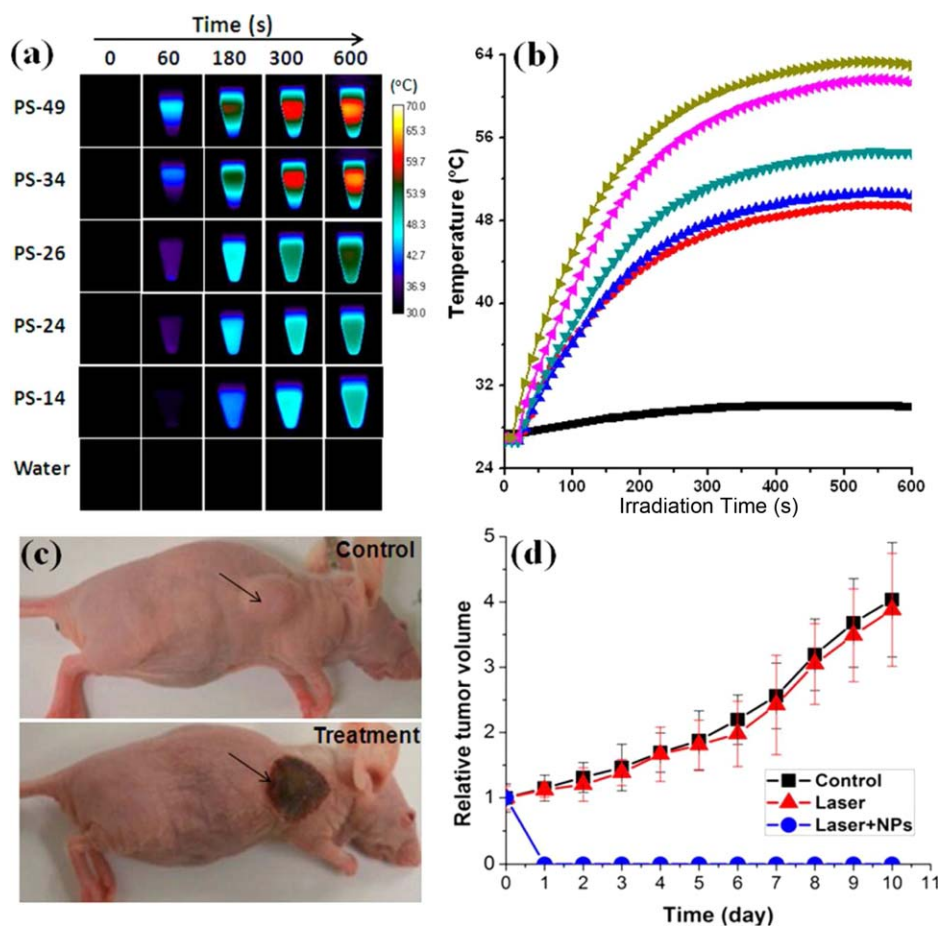


**Figure 8.** (a) Temperature increase induced by the irradiation of Au NP loaded BCMs with an 808-nm laser ( $1 \text{ W/cm}^2$ ). (b) Temperature–time plot of BCMs made from polymers with different molecular weights. (c) Mice bearing 4T1 tumors treated with and without Au NP–BCMs and laser irradiation. (d) Tumor growth curves of different groups of mice after treatment in the presence and absence of Au NP–BCMs. Reproduced with permission from ref. 159. Copyright 2013 American Chemical Society. [Color figure can be viewed in the online issue, which is available at [wileyonlinelibrary.com](http://wileyonlinelibrary.com).]

span the range of potential micellar multifunctionalities. For example, the chemotherapeutic agent DOX and SPIONs [as  $T_2$ -magnetic resonance imaging (MRI) contrast agents] were co-loaded inside PEG-*b*-PCL BCMs functionalized with the monoclonal antibody Cetuximab,<sup>158</sup> and their MRI, therapeutic, and targeting capabilities were tested *in vitro* on epidermoid carcinoma A431 cells. Antibody-functionalized BCMs showed a much larger cellular uptake as visualized by MRI and confocal microscopy when compared to nonfunctionalized ones. Moreover, cellular growth inhibition was also several times higher for Cetuximab immunomicelles. Also, He *et al.*<sup>159</sup> developed Au NP loaded PS–PEG micelles, and the NP plasmon coupling effects within the micelles enabled their successful use as therapeutic agents under NIR light irradiation by means of the photothermal effect while simultaneously allowing the monitoring of cell uptake through multiphoton-absorption-induced luminescence in mice bearing 4T1 tumors (Figure 8). The multifunctionality of BCMs was also cleverly demonstrated by Bae *et al.*,<sup>160</sup> who incorporated three different types of inorganic NPs, 5 nm Au NPs, 4 nm CdSe QDs, and 1–10 nm SPIONs (co-loaded or separately loaded), within spherical and wormlike PS-*b*-PEO BCMs by a hydrodynamic interfacial instabilities based method.

Although the coloaded hybrid micelles have not yet been tested either *in vitro* or *in vivo*, they hold great potential to simultaneously combine three imaging capabilities (MRI, fluorescence imaging, and optical coherence tomography) and three therapeutic modalities (magnetothermal, photodynamic, and photothermal therapies) provided by the loaded SPIONs, QDs, and Au NPs, respectively. The possibilities of combining therapeutic, imaging, and targeting agents are then almost unlimited as long as the partition coefficients of the inorganic cargos and the functional groups of the species to be tagged allow their efficient incorporation into the BCMs without interfering with the acting principle of each element.<sup>26,160–163</sup>

## SUMMARY AND OUTLOOK

Despite the great capabilities of BCMs to encapsulate, release, and target drugs,<sup>164</sup> only a few micellar nanosystems have entered clinical phases for the treatment of several classes of cancers (see Table I). Most of these BCMs combine hydrophilic PEG with PAsp, PGlu, PLA, and PPO blocks within the copolymeric chains and exploit the EPR effect to passively target anti-tumors to reach their respective therapeutic concentrations.

**Table I.** Polymeric Micelles Under Clinical Evaluation

Product	Polymer	Drug	Target	Clinical phase	Mechanism	Company
NK012	PEG-PGlu (SN38)	SN38 (active metabolite of irinotecan)	Breast and small-cell lung cancers	II	Targeting by the EPR effect	Nippon Kayaku Co., Japan
NK105	PEG-PAsp	PTX	Stomach cancer	II	Targeting by EPR	NanoCarrier Co., Japan
NK911	PEG-PAsp (DOX)	DOX	Breast cancer	I	Reduced nephrotoxicity and neurotoxicity	
			Pancreatic, colorectal, leiomyosarcoma, esophageal, and gall bladder cancers	I	Targeting by EPR	Nippon Kayaku Co., Japan
			Breast cancer	II		
SP-1049C	Mixed Pluronic L61 and F127	DOX	Esophageal, gastroesophageal, and gastric cancers	III	Targeting by EPR	Supratek Pharma, Inc., Canada
Genexol-PM	PEG-PLA	PTX	Breast cancer	IV	Functional inhibition of a Pgp efflux pump	
			Pancreatic and non-small-cell lung cancer	II	Targeting by EPR	Samyang Co., Korea
			Improved solubilization and reduction of Chremophor EL toxicity			
NC-4016	Coordination bonds of drug with a PEG-poly(amino acid) copolymer	Oxaliplatin	Colorectal cancer	I	Targeting by EPR	Nanocarrier Co., Japan
NC-6004	Coordination bonds of drug with PEG-PGlu	Cisplatin	Pancreatic cancer	III	Reduced neuropathy	Nanocarrier Co., Japan
			Solid cancer	I/II	Targeting by EPR	
			Solid cancer		Reduced nephrotoxicity and neurotoxicity	
NC-6300/K912	Drug-conjugated through pH-sensitive bond to PEG-PAsp copolymer	Epirubicin	Solid cancer	I	Targeting by EPR	Nanocarrier Co. & Kowa, Japan

Smart polymeric micelles capable of protecting their cargo, selectively reaching the disease site, exclusively entering the affected cells or tissues to exploit specific targeting to overexpressed cell membrane surface receptors, and releasing their cargo by local or remote stimuli are indeed possible nowadays thanks to the versatility and freedom of design provided by copolymer synthesis and self-assembly methods. These new BCM nanodevices are also a convenient and efficacious approach for, for example, preventing premature drug release during circulation and delivering a high concentration of drugs to the action site on demand while allowing the formulation of many existing and new drugs to enhance their therapeutic efficacies and lower their side effects. Moreover, the possibility of combining different elements within BCM nanocarriers, such as therapeutic drugs, antibodies, targeting ligands, imaging contrast agents, and inorganic nanoparticles, would provide new capabilities of considerable importance for an early and sensitive diagnosis of diseases; for optimizing the efficacy of therapeutic interventions through single or combination therapy, in which either internal or external stimuli are used to trigger drug release; and for the monitoring of therapeutic responses that allow the visualization of the efficacy of the intervention in real time and provide the required information for assisting in the decision of whether or not to (dis)continue therapy and whether or not to modify the therapeutic conditions. Hence, these nanosystems should enter widely in clinical trials shortly because they represent part of the frontier of the development of nanomedicine. However, before this occurs, several associated problems with their large-scale production, high economic costs, lack of correlation between the *in vitro* and *in vivo* data, and biotoxicity concerns should be solved. It is necessary to achieve an economic, reproducible, and robust scale up of the BMC-based nanodevices based on simple and reproducible methods that ensure largely monodisperse and stable nanosystems with long shelf lives, sufficient *in vivo* stability, and negligible side effects upon administration. Biocompatibility and biodegradability, which are always major concerns in the establishment of new pharmaceutical formulations, can be easily settled with novel excipients based on BCMs with suitable properties. To the best of our knowledge, only one pH-sensitive polymeric micelle loaded with the antineoplastic drug epirubicin has entered clinical phase I studies for solid tumor treatment.<sup>165</sup>

The ability of some kind of polymeric chains and micelles to interact with cells and, hence, to modify their biological functions needs to be additionally understood to obtain full knowledge about all biochemical processes involved in the cellular pathways that lead to cell death upon micelle administration and subsequent cargo release. In this respect, it has been, for example, suggested that Pluronic, Tetronic, and related more hydrophobic counterparts (e.g., PEO-PSO and reverse PBO-PEO-based triblock copolymers) could inhibit the P-glycoprotein efflux pump and other transporter proteins belonging to the ATP binding cassette by means of membrane fluidization and/or the inhibition of respiratory chains in mitochondria; this will lead to the sensitization of multi-drug-resistant cancer cells.<sup>12,56</sup> Moreover, BCMs could also modify

the transgene expression after transfection and the regulation of different genes, such as CHk1, PLC- $\delta$ , and MDM2 and that of integrin and MMP families, respectively, to offer additional therapeutic effects in angiogenesis and metastasis for cancer treatment.<sup>166</sup>

From the lessons learned from the experience gained in cancer research and the possibility of combining different elements (e.g., drugs, antibodies, nucleic acids, imaging contrast agents, targeting ligands, inorganic NPs), the search for different multifunctionalities within a single polymeric micelle should additionally expand the vast available range of prospective nanodevices to imaging and should look toward treating not only cancerous cells and tissues but also other diseases that target tissues of interest, such as the liver, lungs, bones, stroke sites, and ischemic myocardium, with appropriate targeting ligands to treat diseases such as human immunodeficiency virus, tuberculosis, arthritis, and infarctions, among others, to also make use of alternative administration routes, such as oral,<sup>167,168</sup> ocular,<sup>169</sup> and intranasal routes.<sup>170</sup> For example, BCMs encapsulated with potent antibiotics and decorated with suitable ligands against the cell surface proteins of microbes and parasites or able to protect small RNAs may revolutionize the treatment of many globally important infection or protein-related diseases, respectively. Thus, the utilization of BCMs as nanovehicles to transport and deliver drugs, imaging agents, and other biotherapeutic molecules undoubtedly represents an optimal strategy and promising pathway to solve current clinical needs and afford potential new biomedical applications.

Taken all together, a bright future may be foreseen for BCM-based nanodevices, especially for stimuli-responsive and multifunctional micellar-based nanocarriers. Many drugs that had failed previously because of formulation issues or toxicity issues may possibly be resurrected by the incorporation and adoption of stimuli-responsive nanocarrier technology for efficient delivery.

## ACKNOWLEDGMENTS

The authors thank the Ministry of Economy and Competitiveness and Xunta de Galicia for research projects MAT 2013-40971-R and EM2013-046, respectively. One of the authors (S.B.) greatly acknowledges the Ministry of Economy and Competitiveness for her Ramon y Cajal fellowship. Another author (A.T.) acknowledges the National Council of Science and Technology of Mexico for his Repatriation Program fellowship (contract grant number 232567).

## REFERENCES

1. Dong, R.; Zhou, Y.; Huang, X.; Zhu, X.; Lu, Y.; Shen, J. *Adv. Mater.* **2015**, *27*, 498.
2. Bertrand, C.; Wu, J.; Kamaly, N.; Farokhad, O. C. *Adv. Drug Delivery Rev.* **2014**, *66*, 2.
3. Sun, T.; Zhang, Y. S.; Pang, B.; Hyun, D. C.; Yang, M.; Xia, Y. *Angew. Chem. Int. Ed.* **2014**, *53*, 12320.
4. Plapied, L.; Duhem, N.; des Rieux, A.; Pr eat, V. *Curr. Opin. Colloid Interface Sci.* **2011**, *16*, 228.



5. Miyata, K.; Christie, R. J.; Kataoka, K. *React. Funct. Polym.* **2011**, *71*, 227.
6. Duncan, R.; Vicent, M. J. *Adv. Drug Delivery Rev.* **2013**, *65*, 60.
7. Osada, K.; Christie, R. J.; Kataoka, K. J. R. *Soc. Interface* **2009**, *6*, S325.
8. Bae, Y.; Kataoka, K. *Adv. Drug Delivery Rev.* **2009**, *61*, 768.
9. Gong, J.; Chen, M.; Zheng, Y.; Wang, S.; Wang, Y. J. *Controlled Release* **2012**, *159*, 312.
10. Su, Y.; Hu, Y.; Du, Y.; Huang, X.; He, J.; You, J.; Yuan, H.; Hu, F. *Mol. Pharm.* **2015**, *12*, 1193.
11. Chuanoi, S.; Anraku, Y.; Hori, M.; Kishimura, A.; Kataoka, K. *Biomacromolecules* **2014**, *15*, 2389.
12. Batrakova, E. V.; Kabanov, A. V. *J. Controlled Release* **2008**, *130*, 98.
13. Alvarez-Lorenzo, C.; Rey-Rico, A.; Sosnik, A.; Taboada, P.; Concheiro, A. *Front. Biosci.* **2010**, *E2*, 424.
14. Booth, C.; Attwood, D.; Price, C. *Phys. Chem. Chem. Phys.* **2006**, *8*, 3612.
15. Cambón, A.; Barbosa, S.; Rey-Rico, A.; Figueroa-Ochoa, E. B.; Soltero, J. F. A.; Yeates, S. G.; Alvarez-Lorenzo, C.; Concheiro, A.; Taboada, P.; Mosquera, V. *J. Colloid Interface Sci.* **2012**, *387*, 275.
16. Taboada, P.; Velasquez, G.; Barbosa, S.; Yang, Z.; Nixon, S. K.; Zhengyuan, Z.; Heatley, F.; Ashford, M.; Mosquera, V.; Attwood, D.; Booth, C. *Langmuir* **2006**, *22*, 7465.
17. Xu, W.; Burke, J. E.; Pilla, S.; Chen, H.; Jaskula-Sztul, R.; Gong, S. *Nanoscale* **2013**, *5*, 9924.
18. Koyamatsu, Y.; Hirono, T.; Kakizawa, Y.; Okano, F.; Takarada, T.; Maeda, M. *J. Controlled Release* **2013**, *173*, 89.
19. Veeren, A.; Bhaw-Luximon, A.; Jhurry, D. *Eur. Polym. J.* **2013**, *49*, 3034.
20. Jia, M.; Ren, T.; Wang, A.; Yuan, W.; Ren, J. *J. Appl. Polym. Sci.* **2014**, *131*, 40097/1.
21. Salzano, G.; Riehle, R.; Navarro, G.; Perche, E.; De Rosa, G.; Torchilin, V. P. *Cancer Lett.* **2014**, *343*, 224.
22. Kim, H. J.; Miyata, K.; Nomoto, T.; Zheng, M.; Kim, A.; Liu, X.; Cabral, H.; Christie, R. J.; Nishiyama, N.; Kataoka, K. *Biomaterials* **2014**, *35*, 4548.
23. Zinn, T.; Willner, L.; Lund, R.; Pipich, V.; Appavou, M.-S.; Richter, D. *Soft Matter* **2014**, *10*, 5212.
24. Bailly, N.; Thomas, M.; Klumperman, B. *Biomacromolecules* **2012**, *13*, 4109.
25. Han, Y.; He, Z.; Schulz, A.; Bronich, T. K.; Jordan, R.; Luxenhofer, R.; Kabanov, A. V. *Mol. Pharm.* **2012**, *9*, 2302.
26. Kim, D.-H.; Vitol, E. A.; Liu, J.; Balasubramanian, S.; Gosztola, D. J.; Cohen, E. E.; Novosad, V.; Rozhkova, E. A. *Langmuir* **2013**, *29*, 7425.
27. Yu, Q.; Dong, C.; Zhang, J.; Shi, J.; Jia, B.; Wang, F.; Gan, Z. *Polym. Chem.* **2014**, *5*, 5617.
28. Salmaso, S.; Caliceti, P. *J. Drug Delivery* **2013**, *2013*, 1.
29. Bromberg, L. In *Handbook of Surfaces and Interfaces of Materials*; Nalwa, H. S., Ed.; Academic: Burlington, MA, **2001**; Chapter 7, p 369.
30. He, C.; Kim, S. W.; Lee, D. S. *J. Controlled Release* **2008**, *127*, 189.
31. Madhavan, P.; Peinemann, K. V.; Nunes, S. P. *ACS Appl. Mater. Interfaces* **2013**, *5*, 7152.
32. Liu, Y.; Wang, X. *Polym. Chem.* **2012**, *3*, 2632.
33. Qu, S.; Shen, L.; Chai, Z.; Jing, C.; Zhang, Y.; An, Y.; Shi, L. *ACS Appl. Mater. Interfaces* **2014**, *6*, 19207.
34. Can, A.; Hoepfener, S.; Guillet, P.; Gohy, J.-F.; Hoogenboom, R.; Schubert, U. S. *J. Polym. Sci. Part A: Polym. Chem.* **2011**, *49*, 3681.
35. Yu, L.; Yao, L.; You, J.; Guo, Y.; Yang, L. *J. Appl. Polym. Sci.* **2014**, *131*, 39623/1.
36. Laruelle, G.; Nicol, E.; Ameduri, B.; Tassin, J.-F.; Ajellal, N. *J. Polym. Sci. Part A: Polym. Chem.* **2011**, *49*, 3960.
37. Zhao, Z.-X.; Gao, S.-Y.; Wang, J.-C.; Chen, C.-J.; Zhao, E.-Y.; Hou, W.-J.; Feng, Q.; Gao, L.-Y.; Liu, X.-Y.; Zhang, L.-R.; Zhang, Q. *Biomaterials* **2012**, *33*, 6793.
38. Ponta, A.; Bae, Y. *Pharm. Res.* **2010**, *27*, 2330.
39. Zhang, W.; Jiang, W.; Zhang, D.; Bai, G.; Lou, P.; Hu, Z. *Polym. Chem.* **2015**, *6*, 2274.
40. Taboada, P.; Barbosa, S.; Concheiro, A.; Alvarez-Lorenzo, C. *Soft Nanoparticles for Biomedical Applications*; RSC: London, **2014**; Chapter 5, p 157.
41. Liu, X.; Tian, Z.; Chen, C.; Allcock, H. R. *Polym. Chem.* **2013**, *4*, 1115.
42. Cambón, A.; Figueroa-Ochoa, E.; Blanco, M.; Barbosa, S.; Soltero, J. F. A.; Taboada, P.; Mosquera, V. *RSC Adv.* **2014**, *4*, 60484.
43. Landazuri, G.; Fernandez, V. V. A.; Soltero, J. F. A.; Rharbi, Y. *J. Phys. Chem. B* **2012**, *116*, 11720.
44. Grubbs, R. B.; Sun, Z. *Chem. Soc. Rev.* **2013**, *42*, 7436.
45. Blanz, A.; Madsen, J.; Battaglia, G.; Ryan, A. J.; Armes, S. P. *J. Am. Chem. Soc.* **2011**, *133*, 16581.
46. Fan, H.; Jin, Z. *Soft Matter* **2014**, *10*, 2848.
47. Presa Soto, A.; Gilroy, J. B.; Winnik, M. A.; Manners, I. *Angew. Chem. Int. Ed.* **2010**, *49*, 8220.
48. Holder, S. J.; Sommerdijk, N. A. J. M. *Polym. Chem.* **2011**, *2*, 1018.
49. Liu, C.; Chen, G.; Sun, H.; Xu, J.; Feng, Y.; Zhang, Z.; Wu, T.; Chen, H. *Small* **2011**, *7*, 2721.
50. Li, X.; Yang, H.; Xu, L.; Fu, X.; Guo, H.; Zhang, X. *Macromol. Chem. Phys.* **2010**, *211*, 297.
51. Denkova, A. G.; Bomans, P. H. H.; Coppers, M.-O.; Sommerdijk, N. A. J. M.; Mendes, E. *Soft Matter* **2011**, *7*, 6622.
52. Rösler, A.; Vandermeulen, G. W. M.; Klok, H.-A. *Adv. Drug Delivery Rev.* **2012**, *64*, 270.
53. Qi, J.; Ma, M. G.; Remsen, E. E.; Clark, K. L.; Wooley, K. L. *J. Am. Chem. Soc.* **2004**, *126*, 6599.
54. Lee, S. C.; Huh, K. M.; Lee, J.; Cho, Y. W.; Galinsky, R. E.; Park, K. *Biomacromolecules* **2006**, *8*, 202.
55. Ribeiro, M. E. N. P.; Vieira, Í. G. P.; Cavalcante, I. M.; Ricardo, N. M. P. S.; Attwood, D.; Yeates, S. G.; Booth, C. *Int. J. Pharm.* **2009**, *378*, 211.

56. Cambón, A.; Rey-Rico, A.; Barbosa, S.; Soltero, J. F. A.; Yeates, S. G.; Brea, J.; Loza, M. I.; Alvarez-Lorenzo, C.; Concheiro, A.; Taboada, P.; Mosquera, V. *J. Controlled Release* **2013**, *167*, 68.
57. Yang, Y.; Pan, D.; Luo, K.; Li, L.; Gu, Z. *Biomaterials* **2013**, *34*, 8430.
58. Cao, W.; Gu, Y.; Meineck, M.; Li, T.; Xu, H. *J. Am. Chem. Soc.* **2014**, *136*, 5132.
59. Huo, H.; Gao, Y.; Wang, Y.; Zhang, J.; Wang, Z.-Y.; Jiang, T.; Wang, S. *J. Colloid Interface Sci.* **2015**, *447*, 8.
60. Djurdjic, B.; Dimchevska, S.; Geskovski, N.; Petrusevska, M.; Gancheva, V.; Georgiev, G.; Petrov, P.; Goracinova, K. *J. Biomater. Appl.* **2015**, *29*, 867.
61. Cambón, A.; Rey-Rico, A.; Mistry, D.; Brea, J.; Loza, M. I.; Attwood, D.; Barbosa, S.; Alvarez-Lorenzo, C.; Concheiro, A.; Taboada, P.; Mosquera, V. *Int. J. Pharm.* **2013**, *445*, 47.
62. Prazeres, T. J. V.; Beija, M.; Fernandes, F. V.; Marcelino, P. G. A.; Farinha, J. P. S.; Martinho, J. M. G. *Inorg. Chim. Acta* **2012**, *381*, 181.
63. Attwood, D.; Mosquera, V.; García, M.; Suárez, M. J.; Sarmiento, F. *J. Colloid Interface Sci.* **1995**, *172*, 137.
64. Del Río, J. M.; Prieto, G.; Sarmineto, F.; Mosquera, V. *Langmuir* **1995**, *11*, 1511.
65. Hait, S. K.; Moulik, S. P. *J. Surf. Deterg.* **2001**, *4*, 303.
66. Chiappetta, D. A.; Alvarez-Lorenzo, C.; Rey-Rico, A.; Taboada, P.; Concheiro, A.; Sosnik, A. *Eur. J. Pharm. Biopharm.* **2010**, *76*, 24.
67. Elsabahy, M.; Perron, M.-È.; Bertrand, N.; Yu, G.-E.; Leroux, J.-C. *Biomacromolecules* **2007**, *8*, 2250.
68. Bromberg, L.; Magner, E. *Langmuir* **1999**, *15*, 6792.
69. Yang, Z.; Crothers, M.; Ricardo, N. M. P. S.; Chaibundit, C.; Taboada, P.; Mosquera, V.; Kelarakis, A.; Havredaki, V.; Martini, L.; Valder, C.; Collett, J. H.; Attwood, D.; Heatley, F.; Booth, C. *Langmuir* **2003**, *19*, 943.
70. Li, Y.; Xiao, K.; Zhu, W.; Deng, W.; Lam, K. S. *Adv. Drug Delivery Rev.* **2014**, *66*, 58.
71. van Nostrum, C. F. *Soft Matter* **2011**, *7*, 3246.
72. O'Reilly, R. K.; Hawker, C. J.; Wooley, K. L. *Chem. Soc. Rev.* **2006**, *35*, 1068.
73. Modi, S.; Prakash Jain, J.; Domb, A. J.; Kumar, N. *Curr. Pharm. Des.* **2006**, *12*, 4785.
74. Yokoyama, M. *Expert Opin. Drug Delivery* **2010**, *7*, 145.
75. Torchilin, V. *Adv. Drug Delivery Rev.* **2011**, *63*, 131.
76. Maeda, H.; Bharate, G. Y.; Daruwalla, J. *Eur. J. Pharm. Biopharm.* **2009**, *71*, 409.
77. Kamaly, N.; Xiao, Z.; Valencia, P. M.; Radovic-Moreno, A. F.; Farokhzad, O. C. *Chem. Soc. Rev.* **2012**, *41*, 2971.
78. Nicolas, J.; Mura, S.; Brambilla, D.; Mackiewicz, N.; Couvreur, P. *Chem. Soc. Rev.* **2013**, *42*, 1147.
79. Wu, C.; Chen, T.; Han, D.; You, M.; Peng, L.; Cansiz, S.; Zhu, G.; Li, C.; Xiong, X.; Jimenez, E.; Yang, C. J.; Tan, W. *ACS Nano* **2013**, *7*, 5724.
80. Miura, Y.; Takenaka, T.; Toh, K.; Wu, S.; Nishihara, H.; Kano, M. R.; Ino, Y.; Nomoto, T.; Matsumoto, Y.; Koyama, H.; Cabral, H.; Nishiyama, N.; Kataoka, K. *ACS Nano* **2013**, *7*, 8583.
81. Lou, S.; Gao, S.; Wang, W.; Zhang, M.; Zhang, J.; Wang, C.; Li, C.; Kong, D.; Zhao, Q. *Nanoscale* **2015**, *7*, 3137.
82. Hoang, B.; Ekdawi, S. N.; Reilly, R. M.; Allen, C. *Mol. Pharm.* **2013**, *10*, 4229.
83. Ao, L.; Wang, B.; Liu, P.; Huang, L.; Yue, C.; Gao, D.; Wu, C.; Su, W. *Nanoscale* **2014**, *6*, 10710.
84. Ge, Z.; Liu, S. *Chem. Soc. Rev.* **2013**, *42*, 7289.
85. Hamidi, M.; Shahbazi, M.-A.; Rostamizadeh, K. *Macromol. Biosci.* **2012**, *12*, 144.
86. Yu, C.; Gao, C.; Lu, S.; Chen, C.; Yang, J.; Di, X.; Liu, M. *Colloids Surf. B* **2013**, *115*, 331.
87. Guo, X.; Shi, C.; Wang, J.; Di, S.; Zhou, S. *Biomaterials* **2013**, *34*, 4544.
88. Wang, X.; Li, S.; Wan, Z.; Quan, Z.; Tan, Q. *Int. J. Pharm.* **2014**, *463*, 81.
89. Gao, C.; Li, Q.; Cui, Y.; Huo, F.; Li, S.; Su, Y.; Zhang, W. *J. Polym. Sci. Part A: Polym. Chem.* **2014**, *52*, 2155.
90. Wang, C.; Kang, Y.; Liu, K.; Li, Z.; Wang, Z.; Zhang, X. *Polym. Chem.* **2012**, *3*, 3056.
91. Shao, W.; Miao, K.; Liu, H.; Ye, C.; Du, J.; Zhao, Y. *Polym. Chem.* **2013**, *4*, 3398.
92. Shi, C.; Guo, X.; Qu, Q.; Tang, Z.; Wang, Y.; Zhou, S. *Biomaterials* **2014**, *35*, 8711.
93. Kumar, S.; Allard, J.-F.; Morris, D.; Dory, Y. L.; Lepage, M.; Zhao, Y. *J. Mater. Chem.* **2012**, *22*, 7252.
94. Jin, Q.; Cai, T.; Han, H.; Wang, H.; Wang, Y.; Ji, J. *Macromol. Rapid Commun.* **2014**, *35*, 1372.
95. Yin, T.; Wang, P.; Li, J.; Zheng, R.; Zheng, B.; Cheng, D.; Li, R.; Lai, J.; Shuai, X. *Biomaterials* **2013**, *34*, 4532.
96. Glover, A. L.; Bennett, J. B.; Pritchett, J. S.; Nikles, S. M.; Nikles, D. E.; Nikles, J. A.; Brazel, C. S. *IEEE Trans. Magn.* **2013**, *49*, 231.
97. Pearson, S.; Scarano, W.; Stenzel, M. H. *Chem. Commun.* **2012**, *48*, 4695.
98. Mura, S.; Nicolas, J.; Couvreur, P. *Nat. Mater.* **2013**, *12*, 991.
99. Smart Materials for Drug Delivery; Alvarez-Lorenzo, C., Concheiro, A., Eds.; Royal Society of Chemistry: Cambridge, United Kingdom, **2013**.
100. Zhang, Q.; Re Ko, N.; Kwon Oh, J. *Chem. Commun.* **2012**, *48*, 7542.
101. Gohy, J.-F.; Zhao, Y. *Chem. Soc. Rev.* **2013**, *42*, 7117.
102. Washington, N.; Washington, C.; Wilson, C. G. *Physiological Pharmaceutics: Barriers to Drug Absorption*; Taylor & Francis: London, **2001**; Chapters 5 and 6, p 83.
103. Kraut, J. A.; Madias, N. E. *Nat. Rev. Nephrol.* **2010**, *6*, 274.
104. Schneider, L.; Korber, A.; Grabbe, S.; Dissemmond, J. *Arch. Dermatol. Res.* **2007**, *298*, 413.
105. Felber, A. E.; Dufresne, M. H.; Leroux, J. C. *Adv. Drug Delivery Rev.* **2012**, *64*, 979.

106. Kim, M. S.; Hwang, S. J.; Han, J. K.; Choi, E. K.; Park, H. J.; Kim, J. S.; Lee, D. S. *Macromol. Rapid Commun.* **2006**, *27*, 447.
107. Warnant, J.; Marcotte, N.; Reboul, J.; Layrac, G.; Aqil, A.; Jérôme, C.; Lerner, D. A.; Gérardin, C. *Anal. Bioanal. Chem.* **2012**, *403*, 1395.
108. Zhang, X.; Liu, B.; Yang, Z.; Zhang, C.; Li, H.; Luo, X.; Luo, H.; Gao, D.; Jiang, Q.; Liu, J.; Jiang, Z. *Colloids Surf. B* **2014**, *115*, 349.
109. Carlsen, A.; Lecommandou, S. *Curr. Opin. Colloid Interface Sci.* **2009**, *14*, 329.
110. Engler, A. C.; Bonner, D. K.; Buss, H. G.; Cheung, E. Y.; Hammond, P. T. *Soft Matter* **2011**, *7*, 5627.
111. Quadir, M. A.; Martin, M.; Hammond, P. T. *Chem. Mater.* **2014**, *26*, 461.
112. Kakkar, D.; Mazzaferro, S.; Thevenot, J.; Schatz, C.; Bhatt, A.; Dwarakanath, B. S.; Singh, H.; Mishra, A. K.; Lecommandoux, S. *Macromol. Biosci.* **2015**, *15*, 124.
113. Sun, T.-M.; Du, J.-Z.; Yao, Y.-D.; Mao, C.-Q.; Dou, S.; Huang, S.-Y.; Zhang, P.-Z.; Leong, K. W.; Song, E.-W.; Wang, J. *ACS Nano* **2011**, *5*, 1483.
114. Luo, Y.-L.; Yu, W.; Xu, F.; Zhang, L.-L. *J. Polym. Sci. Part A: Polym. Chem.* **2012**, *50*, 2053.
115. Sun, X. L.; Tsai, P. C.; Bhat, R.; Bonder, E. M.; Michniak-Kohn, B.; Pietrangelo, A. *J. Mater. Chem. B* **2015**, *3*, 814.
116. Prabakaran, M.; Grailer, J. J.; Steeber, D. A.; Gong, S. *Macromol. Biosci.* **2009**, *9*, 744.
117. Boissiere, O.; Han, D.; Tremblay, L.; Zhao, Y. *Soft Matter* **2011**, *7*, 9410.
118. Son, S.; Shin, E.; Kim, B. S. *Biomacromolecules* **2014**, *15*, 628.
119. Theato, P. *Angew. Chem. Int. Ed.* **2011**, *50*, 5804.
120. Yang, H.; Jia, L.; Wang, Z.; Di-Cicco, A. L.; Lévy, D.; Keller, P. *Macromolecules* **2010**, *44*, 159.
121. Yan, Q.; Xin, Y.; Zhou, R.; Yin, Y.; Yuan, J. *Chem. Commun.* **2011**, *47*, 9594.
122. Jiang, J.; Qi, B.; Lepage, M.; Zhao, Y. *Macromolecules* **2007**, *40*, 790.
123. Gupta, M. K.; Meyer, T. A.; Nelson, C. E.; Duvall, C. L. *J. Controlled Release* **2012**, *162*, 591.
124. Hussein, G. A.; Pitt, W. G.; Christensen, D. A.; Dickinson, D. J. *J. Controlled Release* **2009**, *138*, 45.
125. Hussein, G. A.; Pitt, W. G. *Adv. Drug Delivery Rev.* **2008**, *60*, 1137.
126. Hussein, G. A.; Velluto, D.; Kherbeck, L.; Pitt, W. G.; Hubbell, J. A.; Christensen, D. A. *Colloids Surf. B* **2013**, *101*, 153.
127. Rapoport, N. *Int. J. Hyperthermia* **2012**, *28*, 374.
128. Wan, C. P.; Jackson, J. K.; Pirmoradi, F. N.; Chiao, M.; Burt, H. M. *Ultrasound Med. Biol.* **2012**, *38*, 736.
129. De La Rica, R.; Aili, D.; Stevens, M. M. *Adv. Drug Delivery Rev.* **2012**, *64*, 967.
130. Caponi, P. F.; Uljin, R. V. *Smart Materials for Drug Delivery*; RSC: London, **2013**; Vol. 1, Chapter 9, p 232.
131. Zhu, L.; Perche, F.; Wang, T.; Torchilin, V. P. *Biomaterials* **2014**, *35*, 4213.
132. Harnoy, A. J.; Rosenbaum, I.; Tirosh, E.; Ebenstein, Y.; Shaharabani, R.; Beck, R.; Amir, R. J. *J. Am. Chem. Soc.* **2014**, *136*, 7531.
133. Wang, C.; Chen, Q.; Wang, Z.; Zhang, X. *Angew. Chem. Int. Ed.* **2010**, *49*, 8612.
134. Saito, G.; Swanson, J. A.; Lee, K. D. *Adv. Drug Delivery Rev.* **2003**, *55*, 199.
135. Kurz, T.; Eaton, J. W.; Brunk, U. T. *Antioxidants Redox Signaling* **2009**, *13*, 511.
136. Kuppusamy, P.; Li, H.; Ilangoan, G.; Cardounel, A. J.; Zweier, J. L.; Yamada, K.; Krishna, M. C.; Mitchell, J. B. *Cancer Res.* **2002**, *62*, 307.
137. Cheng, R.; Feng, F.; Meng, F.; Deng, C.; Feijen, J.; Zhong, Z. *J. Controlled Release* **2011**, *152*, 2.
138. Li, Y.; Liu, T.; Zhang, G.; Ge, Z.; Liu, S. *Macromol. Rapid Commun.* **2013**, *35*, 466.
139. Thambi, T.; Yoon, H. Y.; Kim, K.; Kwon, I. C.; Yoo, C. K.; Park, J. H. *Bioconjugate Chem.* **2011**, *22*, 1924.
140. Sun, P.; Zhou, D.; Gan, Z. *J. Controlled Release* **2011**, *155*, 96.
141. Koo, A. N.; Min, K. H.; Lee, H. J.; Lee, S.-U.; Kim, K.; Kwon, I. C.; Cho, S. H.; Jeong, S. Y.; Lee, S. C. *Biomaterials* **2012**, *33*, 1489.
142. Perche, F.; Biswas, S.; Wang, T.; Zhu, L.; Torchilin, V. P. *Angew. Chem. Int. Ed.* **2014**, *53*, 3362.
143. Guo, X.; Shi, C.; Yang, G.; Wang, J.; Cai, Z.; Zhou, S. *Chem. Mater.* **2014**, *26*, 4405.
144. Oerlemans, C.; Bult, W.; Bos, M.; Storm, G.; Nijssen, J. F. W.; Hennink, W. E. *Pharm. Res.* **2010**, *27*, 2569.
145. Alvarez-Lorenzo, C.; Sosnik, A.; Concheiro, A. *Curr. Drug Targets* **2011**, *12*, 1389.
146. Klaikherd, A.; Nagamani, C.; Thayumanavan, S. *J. Am. Chem. Soc.* **2009**, *131*, 4830.
147. Wang, X.; Jiang, G.; Li, X.; Tang, B.; Wei, Z.; Mai, C. *Polym. Chem.* **2013**, *4*, 4574.
148. Chen, W.; Yuan, Y.; Cheng, D.; Chen, J.; Wang, L.; Shuai, X. *Small* **2014**, *10*, 2678.
149. Bastakoti, B. P.; Wu, K. C. W.; Inoue, M.; Yusa, S.-I.; Nakashima, K.; Yamauchi, Y. *Chem. Eur. J.* **2013**, *19*, 4812.
150. Marsat, J.-N.; Stahlhut, F.; Laschewsky, A.; Berlepsch, H.; Böttcher, C. *Colloid Polym. Sci.* **2013**, *291*, 2561.
151. Biswas, S.; Deshpande, P. P.; Navarro, G.; Dodwadkar, N. S.; Torchilin, V. P. *Biomaterials* **2013**, *34*, 1289.
152. Song, W.; Tang, Z.; Zhang, D.; Zhang, Y.; Yu, H.; Li, M.; Lv, S.; Sun, H.; Deng, M.; Chen, X. *Biomaterials* **2014**, *35*, 3005.
153. Chen, G.; Wang, L.; Cordie, T.; Vokoun, C.; Eliceiri, K. W.; Gong, S. *Biomaterials* **2015**, *47*, 41.
154. Saraswathy, M.; Knight, G. T.; Pilla, S.; Ashton, R. S.; Gong, S. *Colloids Surf. B* **2015**, *126*, 590.
155. Jhaveri, A. M.; Torchilin, V. P. *Front. Pharmacol.* **2014**, *5*, 1.
156. Duong, H. H.; Yung, L. Y. *Int. J. Pharm.* **2013**, *454*, 486.



157. Guo, J.; Hong, H.; Chen, G.; Shi, S.; Zheng, Q.; Zhang, Y.; Theuer, C. P.; Barhanrt, T. E.; Cai, W.; Gong, S. *Biomaterials* **2013**, *34*, 8323.
158. Liao, C.; Sun, Q.; Liang, B.; Chen, J.; Shuai, X. *Eur. J. Radiol.* **2011**, *80*, 699.
159. He, J.; Huang, X.; Li, Y.-C.; Liu, Y.; Babu, T.; Aronova, M. A.; Wang, S.; Lu, Z.; Chen, X.; Nie, Z. *J. Am. Chem. Soc.* **2013**, *135*, 7974.
160. Bae, J.; Lawrence, J.; Miesch, C.; Ribbe, A.; Li, W.; Emrick, T.; Zhu, J.; Hayward, R. C. *Adv. Mater.* **2012**, *24*, 2735.
161. Liang, R.; Xu, J.; Li, W.; Liao, Y.; Wang, K.; You, J.; Zhu, J.; Jiang, W. *Macromolecules* **2014**, *48*, 256.
162. Wang, J.; Li, W.; Zhu, J. *Polymer* **2014**, *55*, 1079.
163. Li, W.; Liu, S.; Deng, R.; Wang, J.; Nie, Z.; Zhu, J. *Macromolecules* **2013**, *46*, 2282.
164. Upadhyay, K. K.; Meins, J. F. L.; Misra, A.; Voisin, P.; Bouchaud, V.; Ibarboure, E.; Schatz, C.; Lecommandoux, S. *Biomacromolecules* **2009**, *10*, 2802.
165. Takahashi, A.; Yamamoto, Y.; Yasunaga, M.; Koga, Y.; Kuroda, J.-I.; Takigahira, M.; Harada, M.; Saito, H.; Hayashi, T.; Kato, Y.; Kinoshita, T.; Ohkohchi, N.; Hyodo, I.; Matsumura, Y. *Cancer Sci.* **2013**, *104*, 920.
166. Kabanov, A. V.; Batrakova, E. V.; Sriadibhatla, S.; Yang, Z.; Kelly, D. L.; Alakov, V. Y. *J. Controlled Release* **2005**, *101*, 259.
167. Gaucher, G.; Satturwar, P.; Jones, M.-C.; Furtos, A.; Leroux, J.-C. *Eur. J. Pharm. Biopharm.* **2010**, *76*, 147.
168. Bromberg, L. *J. Controlled Release* **2008**, *128*, 99.
169. Yang, J.; Yan, J.; Zhou, Z.; Amsden, B. G. *Biomacromolecules* **2014**, *15*, 1346.
170. Kanazawa, T. *Med. Devices Evidence Res.* **2015**, *8*, 57.